The Use of Non-Linearity Of Eccentrically Loaded Diagonals in Orthogonal Grid Space Truss

Mostafa Raissi Fard

A Thesis

in

The Faculty of Engineering

Presented in Partial Fulfillment of the Requirements
for the Degree of Master of Engineering at
Concordia University
Montréal, Québec, Canada

September 1983

ABSTRACT

THE USE OF NON-LINEARITY OF ECCENTRICALLY LOADED DIAGONALS IN ORTHOGONAL GRID SPACE TRUSS

Mostafa Raissi Fard

This thesis demonstrates the principles of behaviour of the orthogonal grid space truss with T-shape diagonals.

The load-shortening relationships for eccentrically loaded T-shape struts were studied. Tests were carried out on struts and the results were compared with theoretical relations. The loading range was found to be non-linear and was approximated with two straight lines. The stiffness of the eccentrically loaded struts is considerably less than that of axially loaded struts, and decreases with increasing load.

An existing computer program for trusses with axially loaded diagonals was modified for trusses with eccentrically loaded diagonals, and orthogonal grid space trusses, both corner and boundary supported, were analysed.

Moments and shear forces are more uniformly distributed, and the gradual bowing of the T-shape diagonal, rather than the sudden buckling of axially loaded diagonals, gives trusses a "quasi ductile" behaviour in the elastic range which makes them safer and more predictable to analyse.

To demonstrate the influence of T-shape diagonals on the behaviour of space trusses, a small truss with three compression chords was tested. According to elastic theory, when the diagonals are axially loaded the middle chord carries almost twice the load of the side chords. In the same trusses with T-shape diagonals, the side and middle chords carried almost equal loads.

Bowing of diagonals was clearly visible while the truss was still in its elastic range.

TABLE OF CONTENTS

ACKNOWLEDGEMENTS

First and foremost, I would like to express my deep gratitude and appreciation to Professor C. Marsh for his patient supervision, and his generosity in sharing some of his extensive knowledge with me.

Thanks are also due to the technicians in the structures and Centre for Building Studies Laboratories of Concordia University, especially Mr. R. Lombard and Mr. H. Obermier.

Finally I want to thank Miss Tina Rossi for her encouragement and help.

LIST OF TABLES

LIST OF FIGURES

NOTATIONS

x, y	Cartesian coordinates
b	length of stem
C_1	distance to extreme fibre in compression
C_2	distance to extreme fibre in tension
r	radius of gyration
A	cross-section area of a strut
E	elastic modulus
I	moment of inertia
K	numerical factor
L	length
P	load in struts
P_t, P_c	capacities of struts in tension and compression respectively
P_e	Euler load
δ	shortening of struts
Δ	central deflection of struts in loading range
Δ'	central deflection of struts, at first yield of extreme fibre
Δ''	central deflection of struts, assumption of fully plastic stem
ε	strain
σ	mean axial stress
σ_e	Euler stress
σ_y	yield stress
σ_t	tensile stress
σ_c	compressive stress

CHAPTER I

INTRODUCTION

Through 25 centuries of written history, engineers have shared a problem: safely covering of longer spans with less weight.

The space truss is one of the solutions. There are numerous kinds of space truss, varying in both their behaviour under applied load and the method of analysis required. The double-layer orthogonal grid is the most accepted form and is used widely for covering storage areas, exhibition halls, large span industrial buildings, and sport halls.

The characteristics of double-layer three-dimensional latticed structures used in roofs are as follows:

1) Trusses are highly indeterminate, meaning that buckling of a compression member will not usually lead to collapse of the whole truss.
2) The three-dimensional behaviour of the truss distributes the internal forces in all directions.
3) The trusses possess high flexural rigidity with low weight.
4) The small size of the components simplifies handling, transportation and erection.
5) The space between upper and lower grids can be used for services.

6) There is flexibility in the location of the loading supports.

7) The cost is reasonable and the appearance is pleasing.

Double-layer space trusses are composed of two parallel plane grids, formed by the top and bottom chords, connected by vertical or inclined diagonal members. One of the particular forms of double-layer grids is the orthogonal-grid space truss, which can be be viewed as an assembly of square base pyramids, (Fig. 1.1). The upper and lower chords form square plane grids.

METHODS OF ANALYSIS

1) Elastic analysis and plate analogy, by employing discrete or continuum approaches, have been used for many years, and routine computer programs with useful and simplified manuals are available. These analyses are in general confined to linear elastic behaviour.

2) The ultimate load analyses, which take into account the post-buckling behaviour of struts fall into the following groups:

   a) Elastic - plastic (Fig. 1.2 a) in which members are elastically loaded until yielding or buckling occurs, then change length without any change in the force sustained.

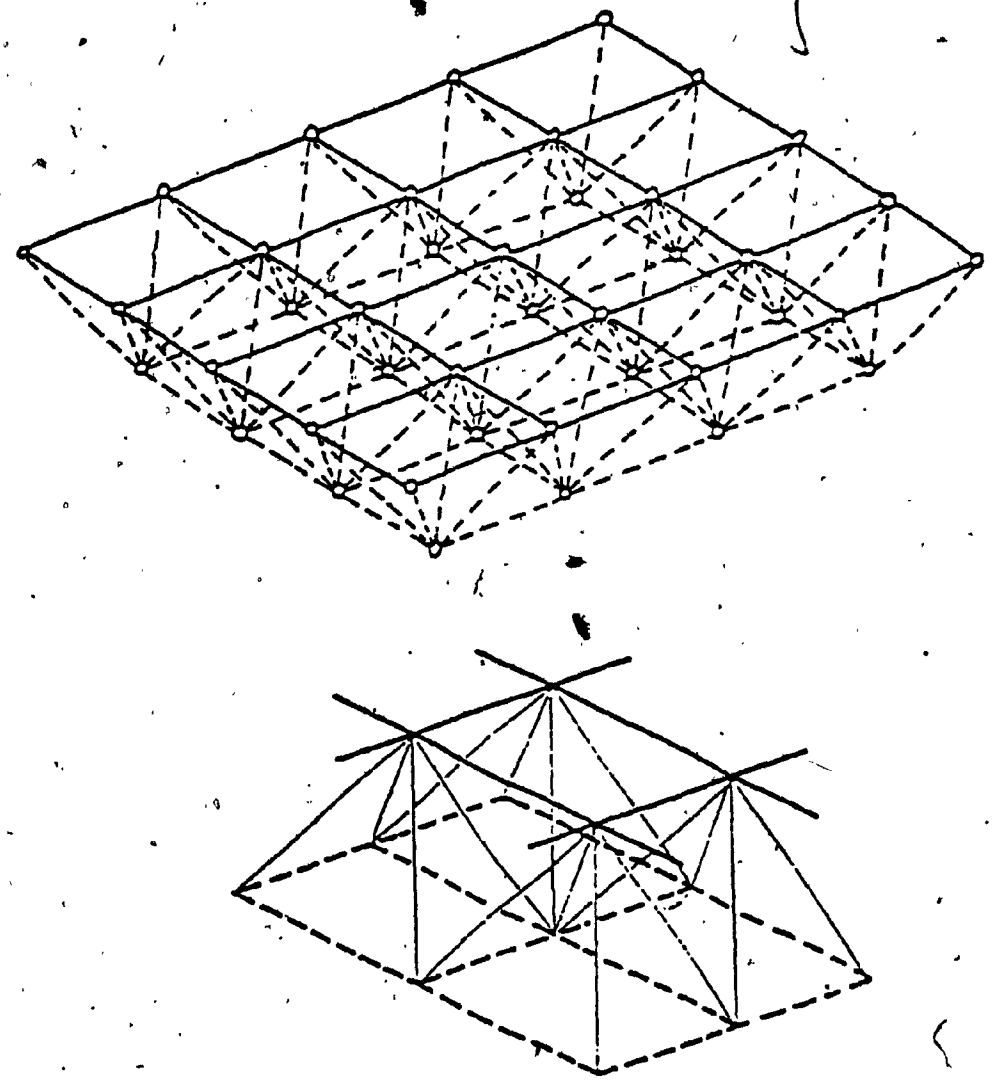

FIG. 1.1 ORTHOGONAL GRID SPACE TRUSS

b) An abrupt drop in load capacities after buckling occurs, (Fig. 1.2 b).

c) Elastic-unloading, in which the loading range is linearly rising till unloading occurs. The unloading phase has been assumed to be either linear, (Fig. 1.2 c) or piece-wise linear (Fig. 1.2 d) as explained in the next chapter.

In orthogonal grid space trusses, compression members in practical and economical range of slenderness are essentially brittle in behaviour. The load-shortening behaviour is more or less linear before the unloading stage occurs.

Eccentricity at the nodes has little influence on the stiffness of the continuous chords. The deflected shape of the chords with regard to the moments at the nodes is shown in fig. (1.3a). Inflection points occur at the mid span and lie on the line which passes through the supports. This compares with a single strut fig. (1.3b) which has a maximum deflection point at the mid span. Chords thus behave as concentric struts, and are brittle in the range of slenderness required for economy. Chord behaviour has been studied by a number of researchers, in particular by Marsh [21] who developed load-shortening relationships for chords (fig. 1.4) in which the compresive capacity of the chords is limited by the first yield.

Nicholas Iliadis, in his thesis [20] gives experimental results for tubular and channel struts which are close to the theory from [21].

The diagonals, which resist the shear force, can be designed to control the forces transferred to the chords and consequently the load capacity of the truss. For concentrically loaded diagonals, again, the failure is brittle, but diagonals are discontinuous and can be eccentrically loaded, which gives them a non-linear load-shortening behaviour. When the force increases, this non-linearity makes them less stiff, thereby transferring force to the adjacent diagonals and hence to adjacent chords. Furthermore the behaviour of the truss is "quasi ductile".

The influence of eccentrically loaded diagonals on the behaviour of orthogonal grid space trusses, and the resulting benefits in the weight and safety are the subject of the present thesis.

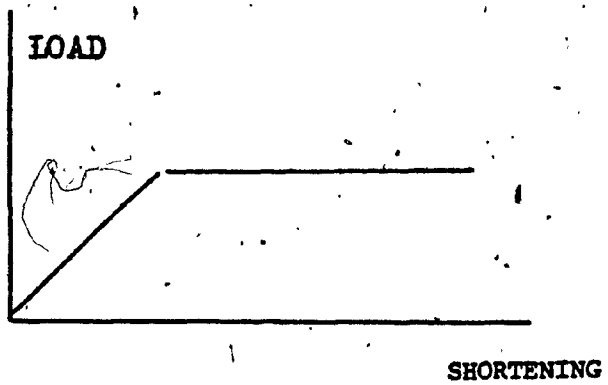

(a) ELASTO -PLASTIC

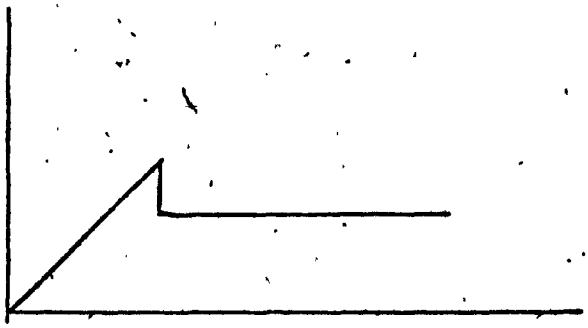

(b) DROP IN LOAD CAPACITY AFTER BUCKLING

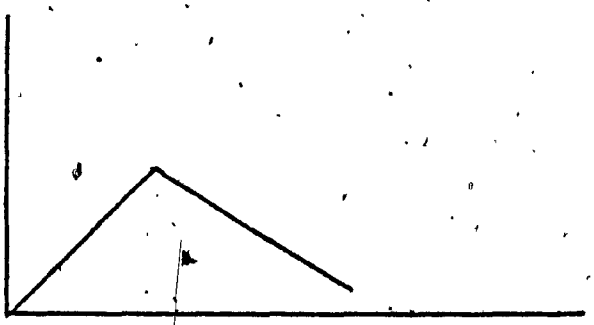

(c)LOAD-UNLOADING LINEAR

(d)LOAD-UNLOADING PIECE WISE LINEAR

FIG. 1.2 IDEALIZED LOAD-SHORTENING RELATIONSHIPS USED FOR STRUTS

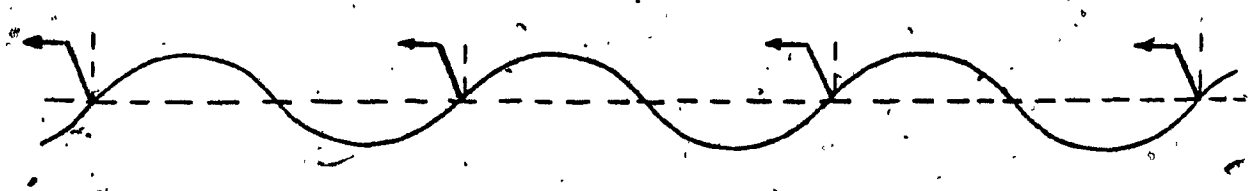

(a)

CONTINUOUS STRUTS

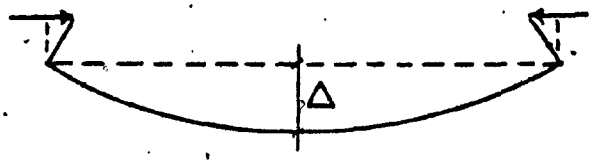

(b)

SINGLE STRUTS

FIG. 1.3 ECCENTRICALLY LOADED MEMBERS

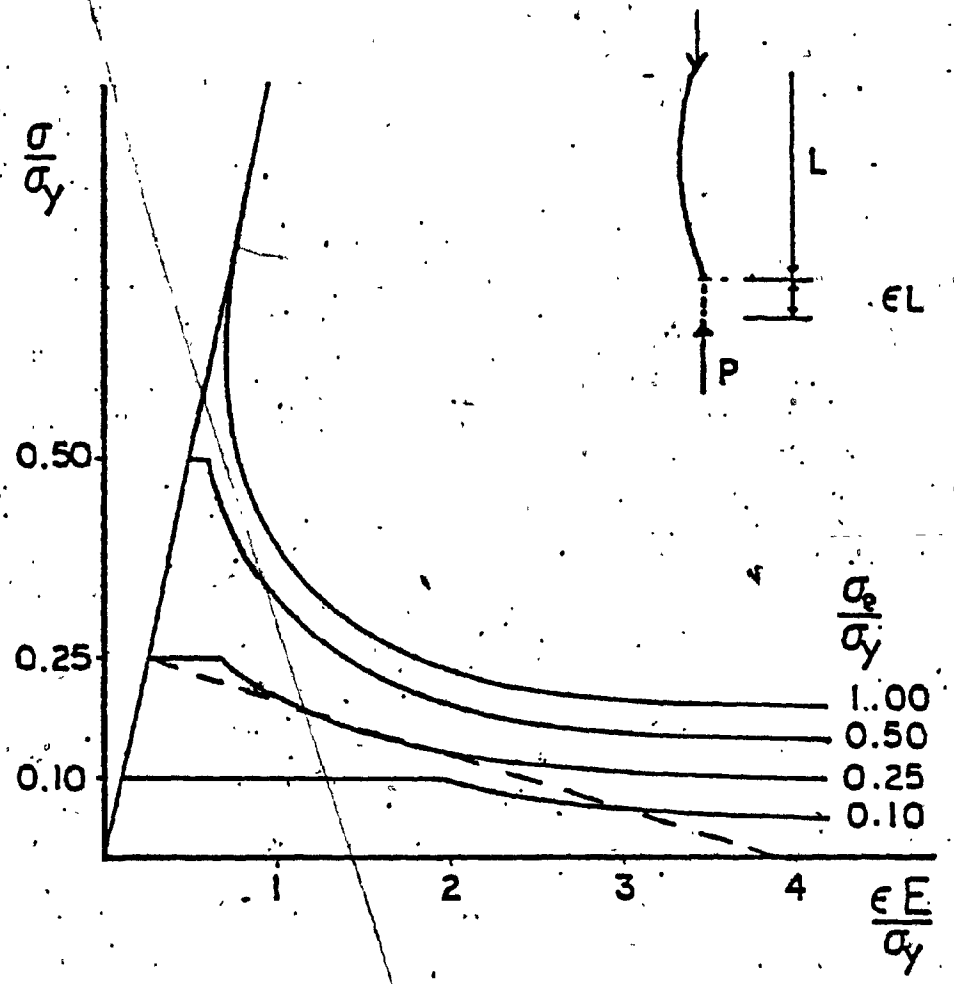

Fig. 1:4 Load Shortening Relationship for Axially Loaded Struts

CHAPTER II

A REVIEW OF THE LITERATURE

There have been two international conferences on space structures, both at the university of Surrey in England, the proceedings of which are comprehensive references on space trusses. In the first, 1966, mainly the elastic behaviour of space trusses was presented. In the second conference [1], 1975, some studies were reported on the ultimate strength of space trusses. Another collection of information on space structures is a 'state-of-the-art report' [2] which is useful as a summary and general review of latticed structures.

Renton [3] compared methods of discrete and continuum analysis. The discrete models, using finite differences, were transformed to differential equations by using Taylor series expansions. Suzuki [4] used the same method as Renton, but instead of Taylor expansion he applied double Fourier Series.

Flower and Schmidt [5] employed differential equations of plates with zero torsional rigidity for space trusses. But they did not investigate the boundary condition or the error caused by different mesh sizes. They indicated that the forces in chords are relatively independent of the rigidity of the diagonals. The equivalent plate analysis can be of lower cost in computer time than the discrete methods.

In another paper [6] Flower and Schmidt discussed a method which converts a truss into an equivalent truss with reduced degrees of freedom, and roughly corresponds to the behaviour of the initial truss.

Dickie and Dunn [7] assumed post buckling behaviour for compression members, such that the buckled members carry 10% of their failure load capacities. For tensile members they assumed a constant load equal to the yielding load. They also considered redistribution of forces in other members. The result of this method was compared with yield line method of analysis. They reported that the initial yield occured at a load factor of 1 and final collapse did not occur until the load factor reached 3.38. This large difference between elastic and ultimate load is excessive and questionable.

Mezzina, Prete and Rosto [8] reported their experimental and elasto-plastic analysis on a double layer grid space truss made of uniform steel tubes welded to node connectors. Their truss failed under a single point load at the centre of the truss, when local punching occured near the load application point. This untypical loading case for space trusses restricts the usefulness of their test.

Schmidt [9] also proposed a plastic design method where tension chords yield before the compression chords buckle. This was compared with the strip method which is used in reinforced concrete design. The

safe and rational application of the strip method requires that the limit moment be maintained at any point in the truss, but buckling may occur before sufficient redistribution of moments. Therefore maximum capacity may not be reached. Also they showed that due to yield in tension a pattern of membrane forces is developed in the truss; these forces make the strip method unsafe to use. However, because of the simplicity of the strip method they have developed a modified method, which is the superposition of bending and membrane effects.

Morgan, Schmidt and Clarkson [11] reported on the behaviour of orthogonal trusses with brittle type strut buckling. The experiment on three identical trusses showed that no reserve of strength exists for the trusses beyond the initial collapse of the compression members. They mentioned that there could be some reserve if the ductile range existed in behaviour of the compression members. They also showed that the post-buckling behaviour of struts is less sensitive to imperfection and eccentricities than the pre-buckling behaviour.

Wolf [12], considering non-linear post-buckling behaviour of struts and using the initial stress method, which was first presented by Zienkiewicz [13], analysed a large space truss in non-linear fashion up to collapse.

Rosen and Schmit [14] in 1979, used a non-linear method to analyse a truss with imperfections. They assumed sinusoidally deflected members

whose stiffness increases in tension and decreases in compression. The stiffness matrix method was used to find the initial buckling load, after which a new axial stiffness was found. A new buckling load was determined and so on, until convergence was reached.

In this method they did not consider post-buckling behaviour of the struts, so the ultimate load capacity of the truss was not predicted.

Schmidt and Grege [15] presented a dual load method that allows highly non-linear member behaviour to be followed. A brittle type of strut and the piecewise linearization of post-buckling behaviour were assumed (Fig. 1.2 d). This method needs repeated assembly and inversion of the stiffness matrix as the stiffness changes.

Morgan, Schmidt and Coulthard [10], investigated space trusses with eccentrically connected members. The influence of continuity and eccentricity in members was considered. They showed that the continuity of members played a significant role in the ultimate load capacity of space trusses. They showed the effect of a gradual build-up of axial forces in the chords from diagonals balances the hazardous effects of eccentricity. They also considered linear pre-buckling behaviour for eccentrically loaded struts, which is questionable. Their model has joint eccentricities whose effects on behaviour of the space truss are too complex to be analysed.

Marsh [16] presented an approximate upper bound analysis method for bending in the orthogonal grid space truss. In this method the energy dissipated in the yielded lines of the truss is equated to the loss of potential energy. He also assumed linear load-unloading load-shortening relationships for struts (the dotted line in Fig. (1.4) whose slope is a function of slenderness ratio). The sequence of the buckling of struts in which the slender chords buckle first optimizes the ultimate capacity.

In this paper [16], Marsh mentioned that unlike concrete slabs and steel plates which have certain shear strengths, the shear strength of space trusses can be varied at will and can control the forces that are transfered to the chords. This concept provides the basis for the ideas developed in this thesis. Advantage is taken of the non-linearity of eccentrically loaded diagonals which, as the load increases, transfer less load to the associated chords than an axially loaded diagonal. The result is a more evenly distributed force system in the chords and an increase in the load carrying capacity of the truss.

CHAPTER III

EFFECT OF ECCENTRICITY ON THE BEHAVIOUR OF STRUTS

3.1 INTRODUCTION

In this chapter the effect of eccentric load on load-shortening behaviour of the T-shape struts is explained. In the elastic range the theory for shortening is based on the secant formula [18]. In the post-yielding (unloading) range, because of the large deformation, it is difficult to determine the exact behaviour of the strut [17]. In the present study lower and upper bounds are established based on first yield and fully plastic stem conditions.

3.2 Theoretical Model for The Loading Range

3.2.1 Load-shortening Relationship

The shortening of a strut under eccentrically applied load for the elastic behaviour has three components.

1. Shortening due to the axial force, δ_1 (Fig. 3.2.A).

$$\delta_1 = \frac{PL}{AE} \qquad (3.1)$$

P = is the applied load

L = length of the strut

A = area

E = modulus of elasticity

II. Shortening due to the tilting of the ends of the strut (Fig. 3.1).

The deflection-moment relationship along the strut is given by:

$$\frac{d^2y}{dx^2} = \frac{M}{EI} = -\frac{Py}{EI} \quad \text{by letting } K = \sqrt{\frac{P}{EI}}$$

$$\frac{d^2y}{dx^2} + yK^2 = 0$$

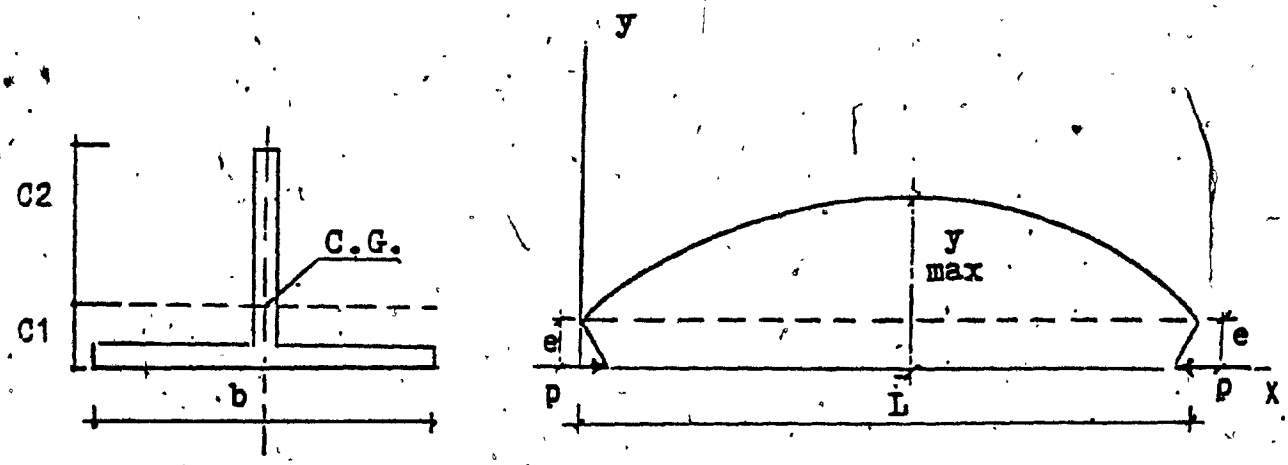

FIG. 3.1 ECCENTRICALLY LOADED T - SHAPE STRUTS

C_1 = distance of the C.G. from extremefibre in compression.

C_2 = distance of the C.G. from extremefibre in tension.

r = radius of gyration.

The general solution for this equation is:

$$y = A \sin Kx + B \cos Kx$$

The boundary conditions are $y(0) = e$

$$y'\left(\frac{L}{2}\right) = 0.$$

Applying these conditions the solutions becomes:

$$y = e\left(\tan \frac{KL}{2} \sin Kx + \cos Kx\right)$$

At the centre of the strut, y is given by:

$$y = e \sec \frac{KL}{2}$$

and deflection $\triangle$ is:

$$\triangle = e\left[\sec\left(\frac{KL}{2}\right) - 1\right] \qquad (3.2)$$

and stresses at the extreme fibres are

$$\left.\begin{aligned} \sigma_c &= -\left(\frac{P}{A} + \frac{MC_1}{I}\right) = -\left(\frac{P}{A} + \frac{P\,y\,C_1}{Ar^2}\right) = -\frac{P}{A}\left(1 + \frac{C_1 y}{r2}\right) \\ \sigma_t &= -\frac{P}{A} + \frac{MC_2}{I} = -\frac{P}{A} + \frac{PyC_2}{Ar^2} = \frac{P}{A}\left(-1 + \frac{yC_2}{r^2}\right) \end{aligned}\right\} (3.3)$$

The slope of the neutral axis along the strut is:

$$y' = eK\left(\tan\frac{KL}{2}\,\mathrm{Cos}\,Kx - \sin Kx\right)$$

The slope at x = 0 is given by:

$$\theta = y'_{(0)} = eK\tan\frac{KL}{2}$$

The shortening due to the tilting of the ends (Fig. 3.2 B) is:

$$\delta_2 = 2\,e\,\theta$$

$$\delta_2 = 2\,e^2K\tan\frac{KL}{2} \qquad \text{and knowing } K = \sqrt{\frac{P}{EI}},\ P_e = \pi^2\frac{EI}{L^2}$$

$$\delta_2 = \frac{PL}{AE}\,\frac{2}{\pi}\left(\frac{e}{r}\right)^2\sqrt{\frac{P_e}{P}}\,\tan\frac{\pi}{2}\sqrt{\frac{P}{P_e}}$$

III. Shortening due to the bow:

Assuming a sine curve for the neutral axis of the strut after bending (Fig. 3.1 c) and by letting Δ be the deflection in the mid span;

$$y = \Delta\sin\frac{\pi x}{L}$$

From the geometry the shortening $\delta 3$ is given by:

$$\delta_3 = \frac{1}{2}\int_0^L (y')^2 dx \qquad \text{and } y' = \frac{\pi}{L}\Delta\,\mathrm{Cos}\,\frac{\pi x}{L}$$

$$\therefore\ \delta_3 = \frac{1}{2}\int_0^L \frac{\pi^2}{L^2}\Delta^2\,\mathrm{Cos}^2\frac{\pi x}{L}\,dx$$

$$\therefore \quad \delta_3 = \frac{\pi^2}{4L}\Delta^2 \qquad (3.4)$$

By using the max deflection Δ from relation (3.2) we have:

$$\delta_3 = \frac{\pi^2}{4L} e^2 \left[\sec\left(\frac{KL}{2}\right) - 1\right]^2$$

The total shortening is

$$\delta = \delta_1 + \delta_2 + \delta_3$$

$$\delta = \frac{PL}{AE} + \frac{PL}{AE}\,\frac{2}{\pi}\,\left(\frac{e}{r}\right)^2 \sqrt{\frac{P_e}{P}}\,\tan\frac{\pi}{2}\sqrt{\frac{P}{P_e}} + 0.25\,\frac{\pi^2}{L}\,e^2\left[\sec\left(\frac{KL}{2}\right) - 1\right]^2$$

Letting $\sigma = \frac{P}{A}$

$$\sigma_e = \frac{P_e}{A} \quad \text{where } P_e = \frac{\pi^2 EA}{\left(\frac{L}{r}\right)^2}$$

$$\varepsilon = \delta/L$$

$$\frac{E\varepsilon}{\sigma_y} = \frac{\sigma}{\sigma_y}\left[1 + \frac{2}{\pi}\left(\frac{e}{r}\right)^2\sqrt{\frac{\sigma_e}{\sigma}}\,\tan\frac{\pi}{2}\sqrt{\frac{\sigma}{\sigma_e}}\right] + 0.25\,\frac{\sigma_e}{\sigma_y}\left(\frac{e}{r}\right)^2\left(\sec\frac{\pi}{2}\sqrt{\frac{\sigma}{\sigma_e}} - 1\right)^2 \qquad (3.5)$$

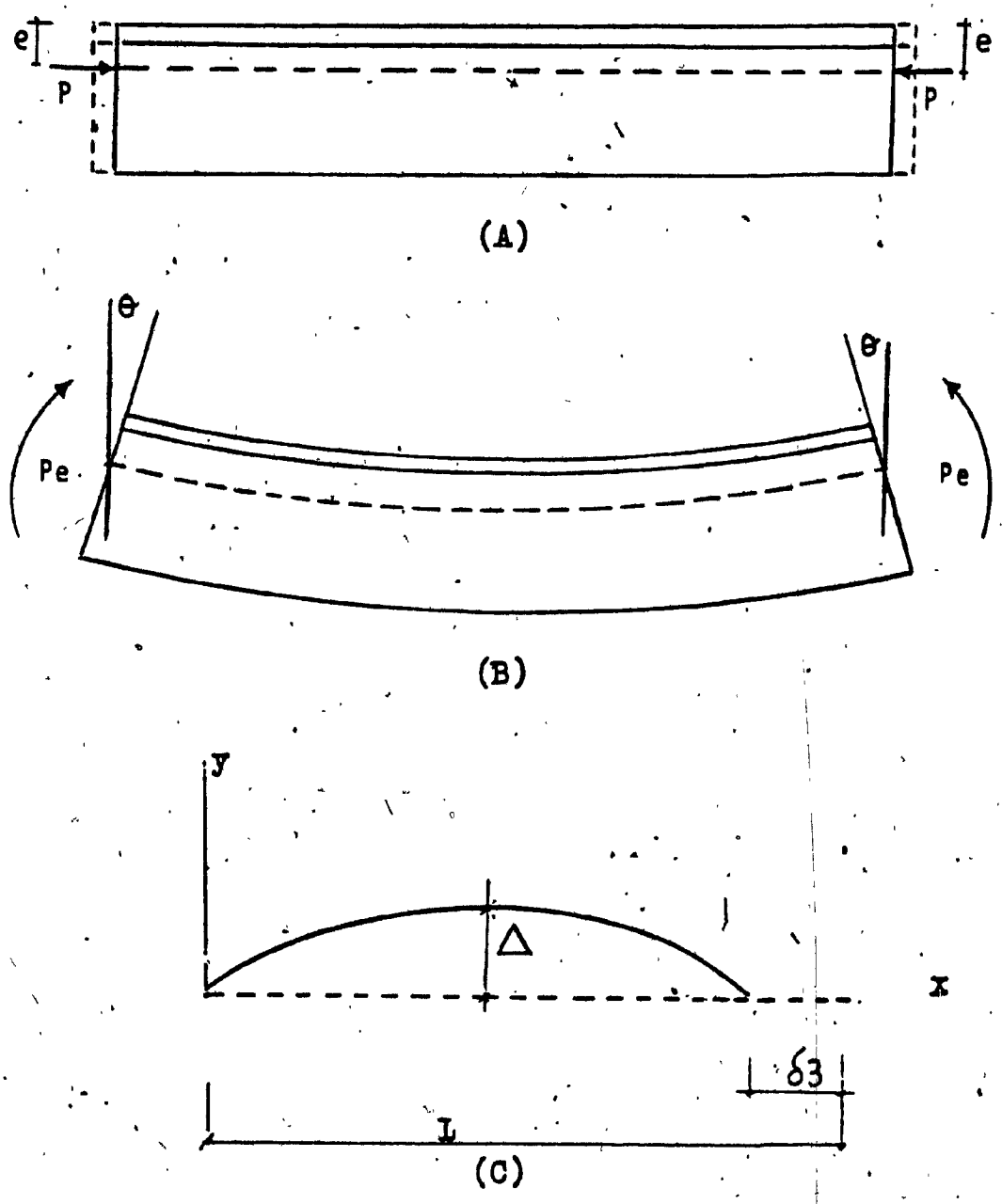

FIG. 3.2 SHORTENING OF A STRUT UNDER ECCENTRIC LOAD

A) SHORTENING DUE TO AXIAL STRESS

B) TILTING OF THE ENDS

C) SHORTENING DUE TO THE BOW

3.2.2 Limiting Compressive Capacity

In practical T-sections which are eccentrically loaded at the flange, the extreme fibre in the stem yields first in tension. In order to show this, a general T-section is analysed. The ratio of the flange to the stem area is variable (f).

The properties of section, when the C.G. is located in the stem (Fig. 3.3) are as follows:

$$A = bt\ (1+f)$$

$$C_1 = \frac{b}{2} \cdot \frac{1}{1+f}$$

$$C_2 = \frac{b}{2} \cdot \frac{2f+1}{1+f}$$

$$I = b^3t\ \left(\frac{1}{12} + \frac{1}{4}\,\frac{f}{1+f}\right)$$

$$r_2 = \frac{b^2}{12}\,\frac{(1+4f)}{(1+f)^2}$$

The tensile and compressive stresses (σ_t, σ_c), assuming $e = C_1$ are:

$$\sigma_t = \frac{P}{A}\left[-1 + \frac{(\Delta+C_1)\ C_2}{r^2}\right]$$

$$\sigma_c = \frac{P}{A}\left[1 + \frac{(\Delta+C_1)}{r^2}\ C_1\right]$$

Tensile stress greater than compressive requires that:

$$\frac{P}{A}\left[-1+\frac{(\Delta+C_1)C_2}{r^2}\right] > \frac{P}{A}\left[1+\frac{(\Delta+C_1)C_1}{r^2}\right]$$

$$\frac{\Delta}{r^2}(C_2-C_1)+\frac{C_1C_2-C_1^2}{r^2} > 2$$

applying the values of C_1 and C_2 we get:

$$\Delta \cdot \frac{6}{b} \cdot \frac{2f(1+f)}{1+4f} + 3\ \frac{2f}{1+4f} > 2$$

$$6\frac{\Delta}{b} f(1+f) + 3f > 1+4f$$

$$6\frac{\Delta}{b} f > 1 \qquad (3.6)$$

For Δ, the value which is obtained only from bending of a member in pure bending is:

$$\Delta = \frac{PeL^2}{8EI}$$

knowing $e = C_1$ and $P_e = \frac{\pi^2 EI}{L^2}$ gives:,

$$\Delta = \frac{P}{P_e} \cdot \frac{\pi^2}{8} \cdot C_1$$

if $P \approx P_e$ then $\Delta \approx C_1$ and (3.6) gives:

$$6\frac{C_1}{b} f > 1$$

$$6 \quad \frac{b}{2} \cdot \frac{1}{1+f} \quad \frac{1}{b} \; f > 1$$

$$f > 0.5$$

meaning if the web is greater than half the length of the stem, tensile yielding occurs first. In practical sections the flange is at least as great as the stem i.e. $f > 1$.

The maximum compressive capacity of the strut is assumed to be that to which causes the extreme tension fibre to yield, i.e:

$$\sigma_y = \sigma\left(-1 + \frac{yC2}{r^2}\right)$$

where $y = e \sec\left(\frac{\pi}{2}\sqrt{\frac{\sigma}{\sigma_e}}\right)$

which gives:

$$\sigma_y = \sigma\left[-1 + \frac{eC2}{r^2} \sec\left(\frac{\pi}{2}\sqrt{\frac{\sigma}{\sigma_e}}\right)\right]$$

σ, the mean axial stress, P/A, is found by trial and error.

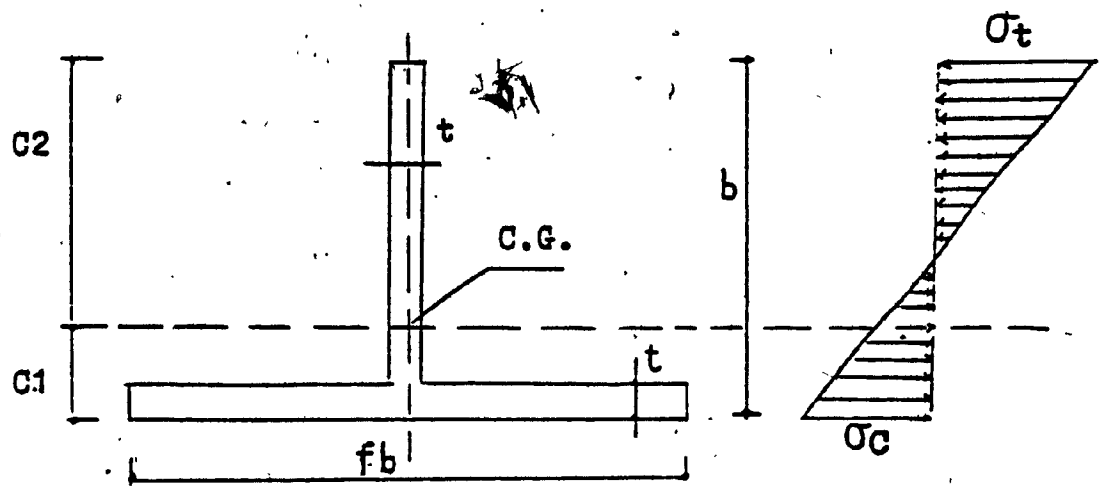

Fig. 3.3 A T-Section, and Stress Distribution

3.3 Unloading Range

I. Lower bound: Assume that only the extreme fibre reaches the yield in tension and other fibres remain elastic (Fig. 3.4a). As deflection increases the load decreases to maintain equilibrium expressed by:

$$\sigma_y = \frac{P}{A}\left[-1 + \frac{(\Delta'+e)C_2}{r^2}\right]$$

$$\frac{\Delta'}{r} = \left(\frac{\sigma_y}{\sigma} + 1\right)(r/C_2) - \frac{e}{r} \qquad (3.7)$$

The compressive stress in the extreme fibre along the strut is given by:

$$\sigma_c = \frac{P}{A}\left[1 + \frac{y\,C_1}{r^2}\right] \quad \text{where } y = e + \Delta' \sin\frac{\pi}{L}x$$

the shortening due to this stress is:

$$\delta_1' = \int_0^L \frac{\sigma_c}{E}\,dx$$

$$\delta_1' = \frac{2}{E}\int_0^{\frac{L}{2}} \frac{P}{A}\left[1 + \left(\Delta' \sin\frac{\pi}{L}x\right)\frac{C_1}{r^2} + \frac{eC_1}{r}\right]dx$$

$$\delta_1' = \frac{\sigma}{E}\left[L + \frac{eC_1}{r^2}L + 2\Delta'\frac{L}{\pi}\frac{C_1}{r_2}\right]$$

$$\delta_1' = \frac{\sigma L}{E}\left[1 + \left(\frac{e}{r}\right)\left(\frac{C_1}{r}\right) + \frac{2}{\pi}\left(\frac{\Delta'}{r}\right)\left(\frac{C_1}{r}\right)\right]$$

Δ' is found from (3.7).

The shortening due to the bow is again:

$$\delta_2'' = \frac{\pi^2 \Delta^2}{4L}$$

The total shortening is:

$$\delta' = \frac{PL}{AE}\left[1 + \left(\frac{e}{r}\right).\left(\frac{c_1}{r}\right) + \frac{2}{\pi}\left(\frac{\Delta'}{r}\right).\left(\frac{c_1}{r}\right)\right] + 0.25\,\frac{\pi^2 \Delta'^2}{L}$$

By dividing both sides by L and multiplying by $\frac{E}{\sigma_y}$ and knowing

$\sigma_e = \frac{\pi^2 E}{\left(\frac{L}{r}\right)^2}$ we get:

$$\frac{\varepsilon E}{\sigma_y} = \frac{\sigma}{\sigma_y}\left[1 + \left(\frac{e}{r}\right).\left(\frac{c_1}{r}\right) + \frac{2}{\pi}\left(\frac{\Delta'}{r}\right).\left(\frac{c_1}{r}\right)\right] + 0.25\,\frac{\sigma_e}{\sigma_y}\left(\frac{\Delta'}{r}\right)^2 \qquad (3.8)$$

where $\varepsilon = \frac{\delta'}{L}$

Using Δ' from (3.7), the relationship between $\frac{\varepsilon E}{\sigma_y}$ and $\frac{\sigma}{\sigma_y}$ for (3.8) is plotted in Fig. 4.4 to 4.6.

II. Upper bound: Assume the stem of the T-section is completely yielded (Fig. 3.4 b). Force equilibrium gives:

$$P = \sigma_f\, fbt - \sigma_y\, bt$$

The area equals $bt(1+f)$ $\therefore \sigma_f = \frac{P}{fbt} + \frac{\sigma_y}{f} = \sigma\,\frac{(1+f)}{f} + \frac{\sigma_y}{f}$

where f is the ratio of the flange to the stem (Fig. 3.4 c) and σ_f is the compressive stress at the centre of the strut.

Moment equilibrium gives:

$$P\,\Delta'' = \frac{(b)^2}{2} t\sigma_y \therefore \Delta'' = \frac{b}{2(1+f)} \frac{\sigma_y}{\sigma}$$

By assuming a parabolic stress variation along the strut (fig. 3.4d), the compressive stress in the flange can be expressed as:

$$\sigma_c = \sigma(1+\frac{eCl}{r^2}) + [\sigma_f - \sigma(1+\frac{eCl}{r^2})]4[\frac{x}{L} - (\frac{x}{L})^2]$$

and the shortening due to this stress, δ_1'', is:

$$\delta_1'' = \int_0^L \frac{\sigma_c}{E}\,dx$$

$$\delta_1'' = \frac{\sigma L}{E}[1 + \frac{1}{3}(\frac{e}{r})(\frac{Cl}{r}) + \frac{2}{3}(\frac{1+f}{f} - \frac{\sigma_y}{f\sigma})]$$

The other component of shortening is due to the bow (relation 3.4):

$$\delta_2'' = \pi^2 \frac{\Delta''^2}{4L}$$

The total shortening for strut with fully plastic stem, δ'', therefore is:

$$\delta'' = \delta_1'' + \delta_2''$$

$$\delta'' = \frac{\sigma L}{E}[\frac{1}{3} + \frac{1}{3}(\frac{e}{r})(\frac{Cl}{r}) + \frac{2}{3}(\frac{1+f}{f} + \frac{\sigma_y}{f\sigma})] + \frac{\pi^2}{4L}[\frac{b}{2(1+f)} \frac{\sigma_y}{\sigma}]^2$$

by using $\sigma_e = \frac{\pi^2 E r^2}{L^2}$, multipling both sides by $\frac{E}{L\sigma_y}$ and letting $\xi = \frac{\Delta''}{L}$

$$\frac{\varepsilon E}{\sigma_y} = \frac{\sigma}{\sigma_y}\left[1 + \frac{1}{3}\left(\frac{e}{r}\right)\left(\frac{C1}{r}\right) + \frac{2}{3f}\left(1 + \frac{\sigma_y}{\sigma}\right)\right] + \frac{1}{16(1+f)^2}\frac{b^2\sigma_e}{r^2\sigma_y}\left(\frac{\sigma_y}{\sigma}\right)^2 \quad (3.9)$$

For given proportions of a T-shape of given length, with a given yield stress and elastic modulus, equation (3.9) gives the effective axial strain ε for each level of mean axial stress σ. The resulting curves are plotted in terms of the non-dimensional function $\frac{\varepsilon E}{\sigma_y}$ and $\frac{\sigma}{\sigma_y}$ in Fig. 4.4 to 4.6.

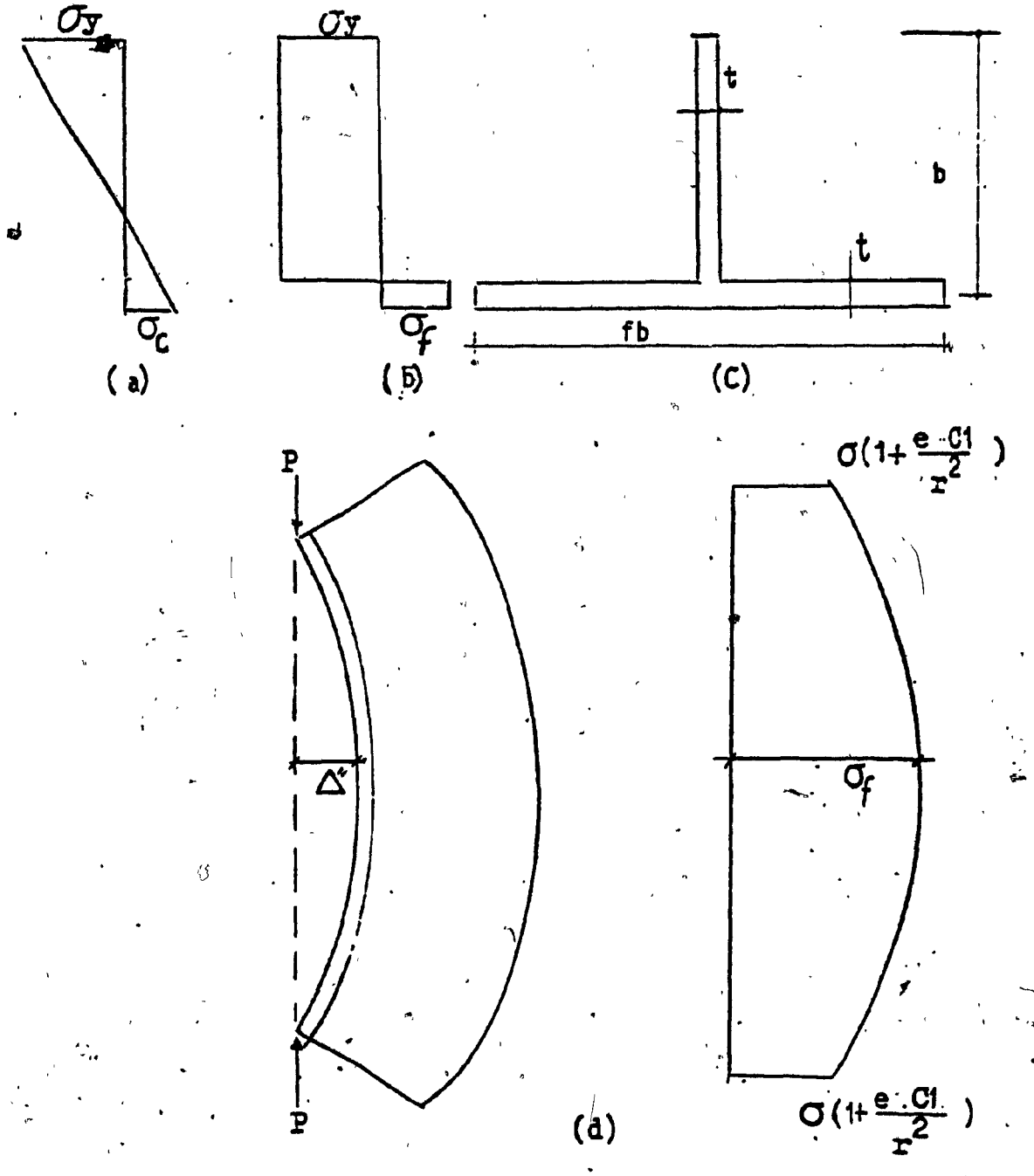

Fig. 3.4 - Stresses for Unloading Stage

a) First yield in tension

b) Fully plastic in stem

c) The T-section, with f as the ratio of the flange to the stem area

d) Stress distribution along the strut for fully plastic stem

CHAPTER IV

ECCENTRICALLY LOADED STRUTS TESTS

4.1 INTRODUCTION

In order to determine the actual behaviour of the eccentrically loaded struts, and to compare this with the theoretical findings, a number of experiments were carried out on T-shape aluminum bars.

4.2 Description of the Struts

The struts tested were 6063-T6 aluminum alloy , with T-shape cross sections in three different slenderness ratios ($\frac{l}{r}$ = 56, 80, 140). Fig. (4.1) shows the shape and dimensions of the cross sections, as well as their geometrical properties. At each end, two bolts were used to attach the web of the bars to 5 mm thick plates, Fig. (4.2). These plates provide pinned ends for bending about the y-axis and fixed end for x-axis bending.

4.3 Material behaviour:

Some of the mechanical properties of aluminum which are defined in [19] are as follows:

- Yield strength, σ_y, the stress at which the material displays a permanent set of 0.2%. The onset of non-linear behaviour is below this stress level and for the alloy

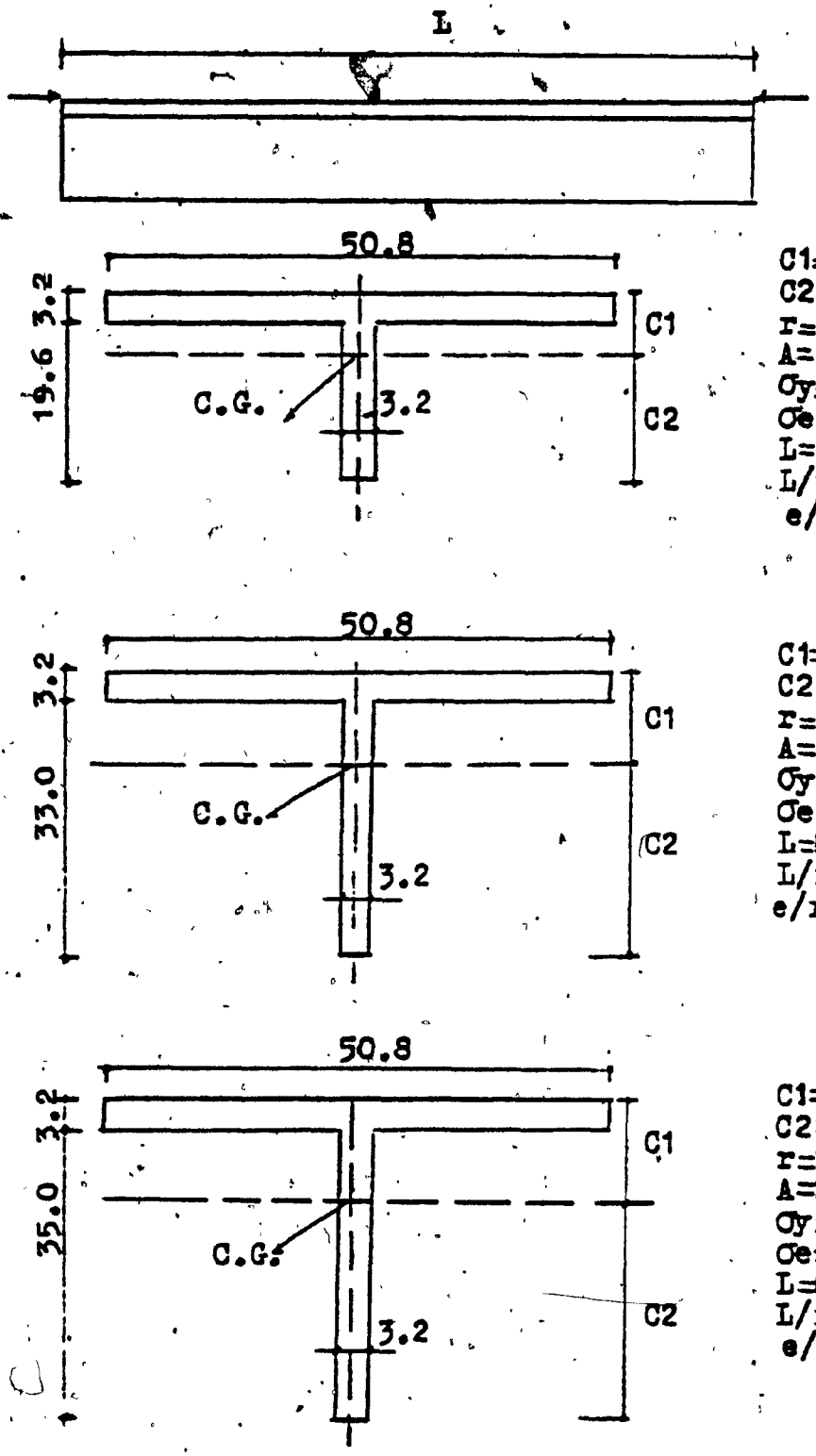

FIG. 4.1 GEOMETRICAL PROPERTIES OF TESTED T-SHAPE STRUTS.

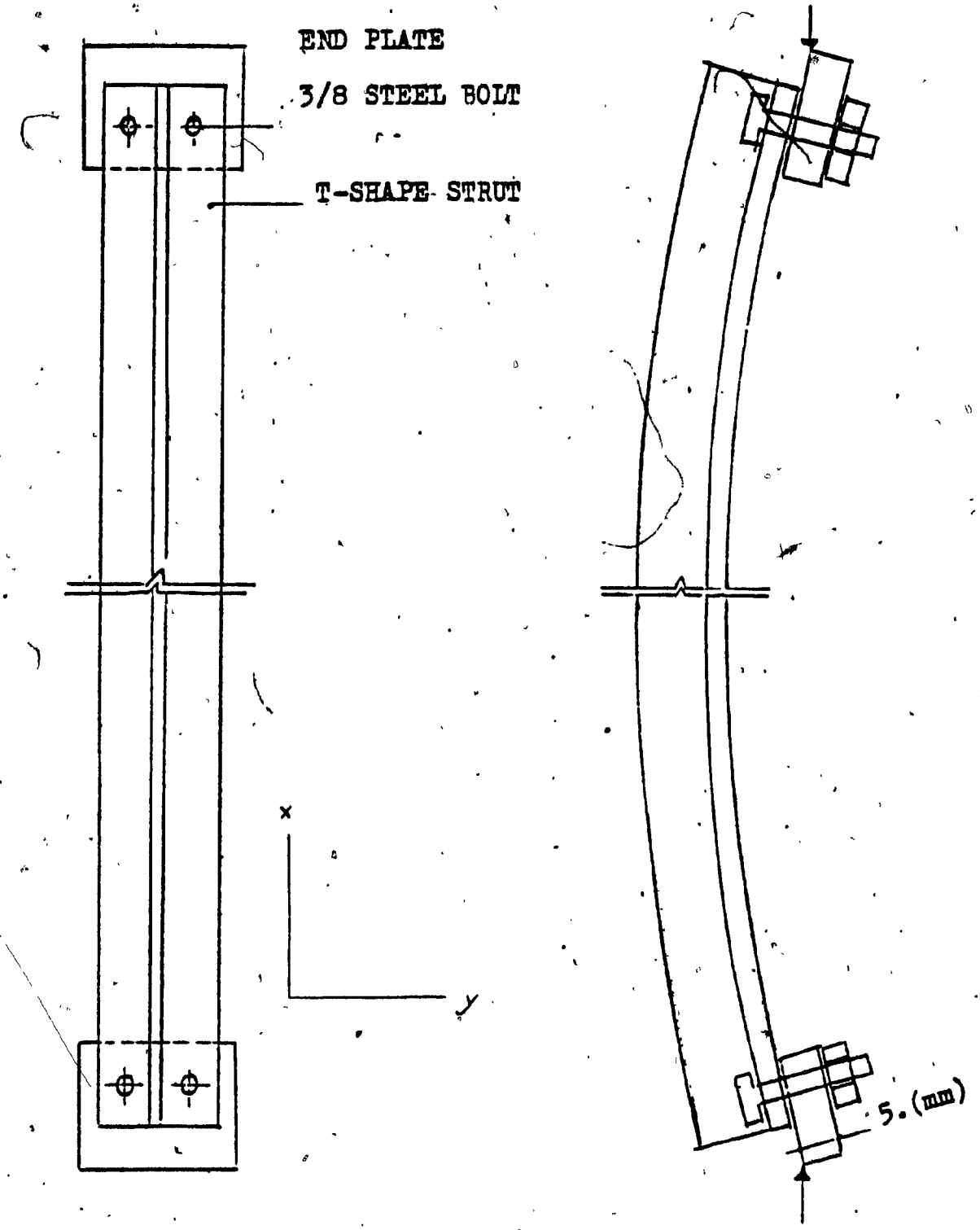

FIG. 4.2 LOCATION OF THE END PLATES AND BOLTS ON STRUTS

used in the tests (6063-T5) the limit of proportionality is approximately 80% of the measured yield stress.

- Ultimate tensile strength, σ_u; the stress obtained by dividing the maximum load by the original cross section of the specimen.
- The elastic modulus E; the slope of the straight line of the stress-strain curve, $E = 7 \times 10^4$ MPa.
- Tangent modulus, the slope of stress-strain curve for stresses above the proportional limit.

The stress-strain curve for aluminum used in this study (6063 -T5) was found experimentally and is shown in Fig. (4.3).

4.4 Instrumentation

Force and shortening measurement: The force was applied by an Instron testing machine. This system has a chart which plots the applied force against the shortening of the strut.

4.5 Test Procedure

The procedure was basically the same for all three specimens. Compression force was applied to the end plates. As the force increased, the shortening (movement of the cross head of machine) was continuously recorded up to the maximum force, and into the unloading phase until rupture occurred in tension.

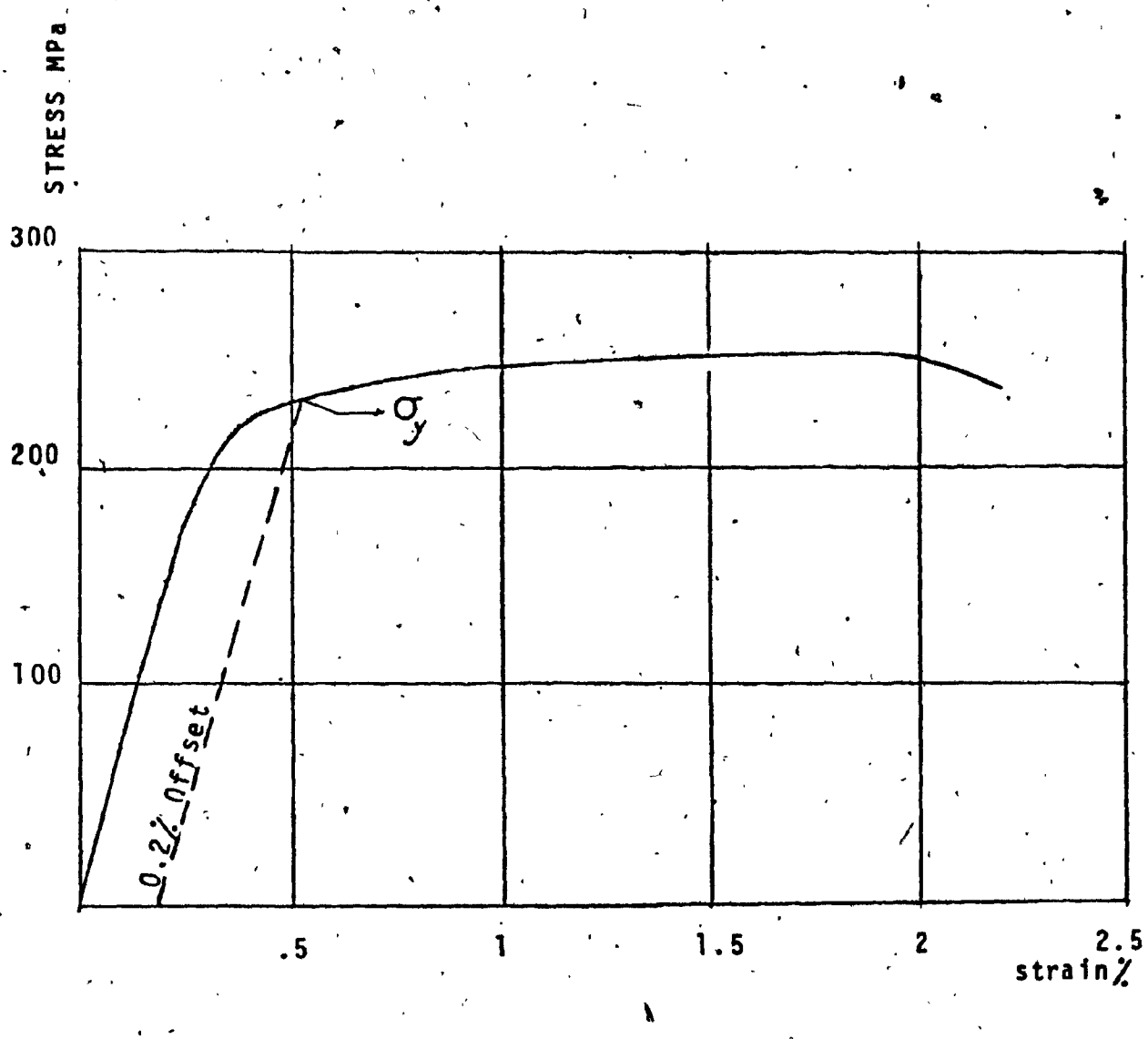

FIG 4.3 STRESS-STRAIN CURVE FOR ALUMINUM ALLOY USED IN TESTS

4.6 Test Results

The load-shortening results obtained from the tests are shown, for different slenderness ratio in Figs. (4.4, 4.5, 4.6). The coordinates are $\frac{\sigma}{\sigma_y}$ and $\frac{\varepsilon E}{\sigma_y}$ which are non-dimensional. The result from the theory (relations 3.8, 3.9) are also shown. The maximum compressive loads, Pmax., are shown in Table 4.1.

Slenderness Ratio L/r	P_{max} / KN	
	Experiment	Theory
140	4.5	5.1
80	13.4	13.6
56	19.5	19.6

TABLE 4.1

Maximum Compressive Capacity of Eccentrically loaded Struts

The non-linear load-shortening behaviour of the struts was observed for all of the struts, but more conspicuously for longer struts. Three regions in the curves are noticable:

I - Loading Phase:

The curve in the loading region showed a small difference between experiment and theory. The experiment gave more shortening than the theory gives.

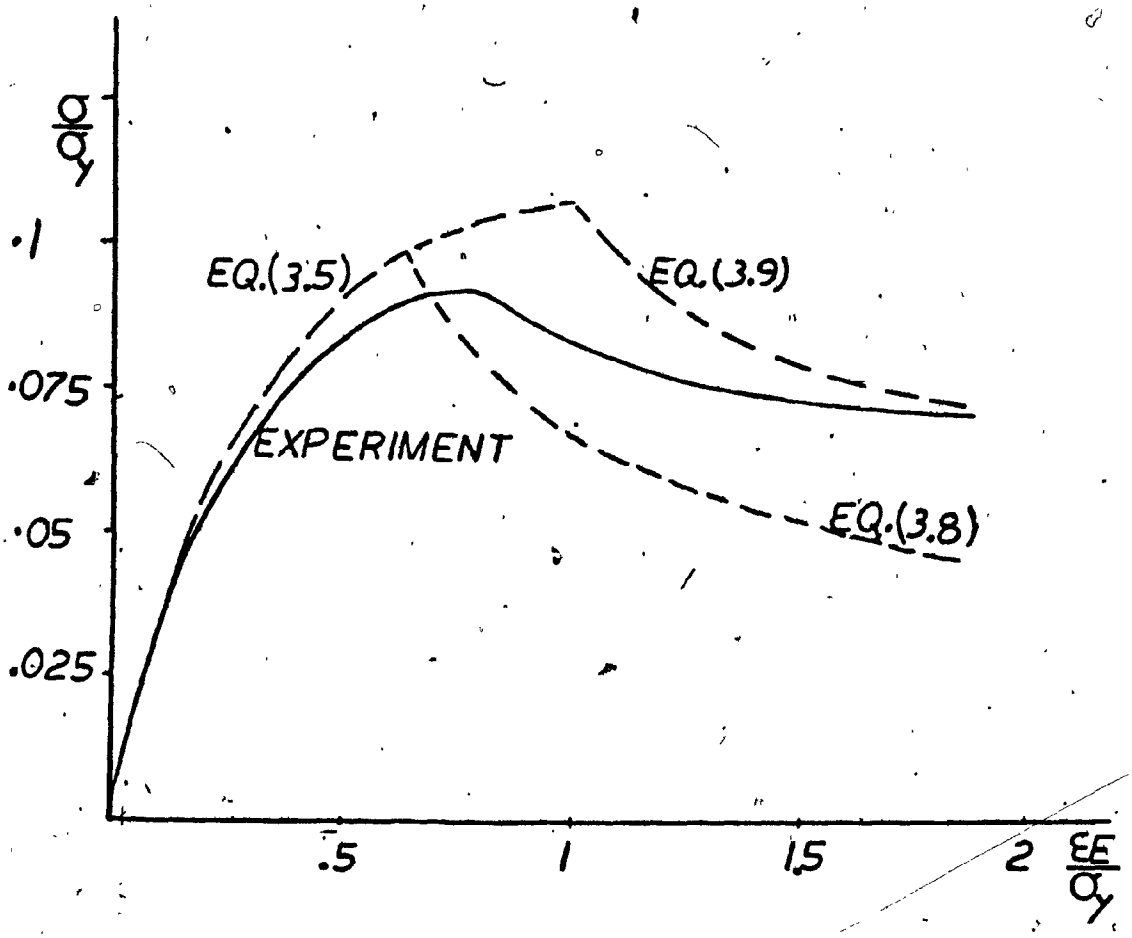

FIG. 4.4 : LOAD-SHORTENING RELATIONSHIPS FOR T-SHAPE STRUTS (L/r = 140)

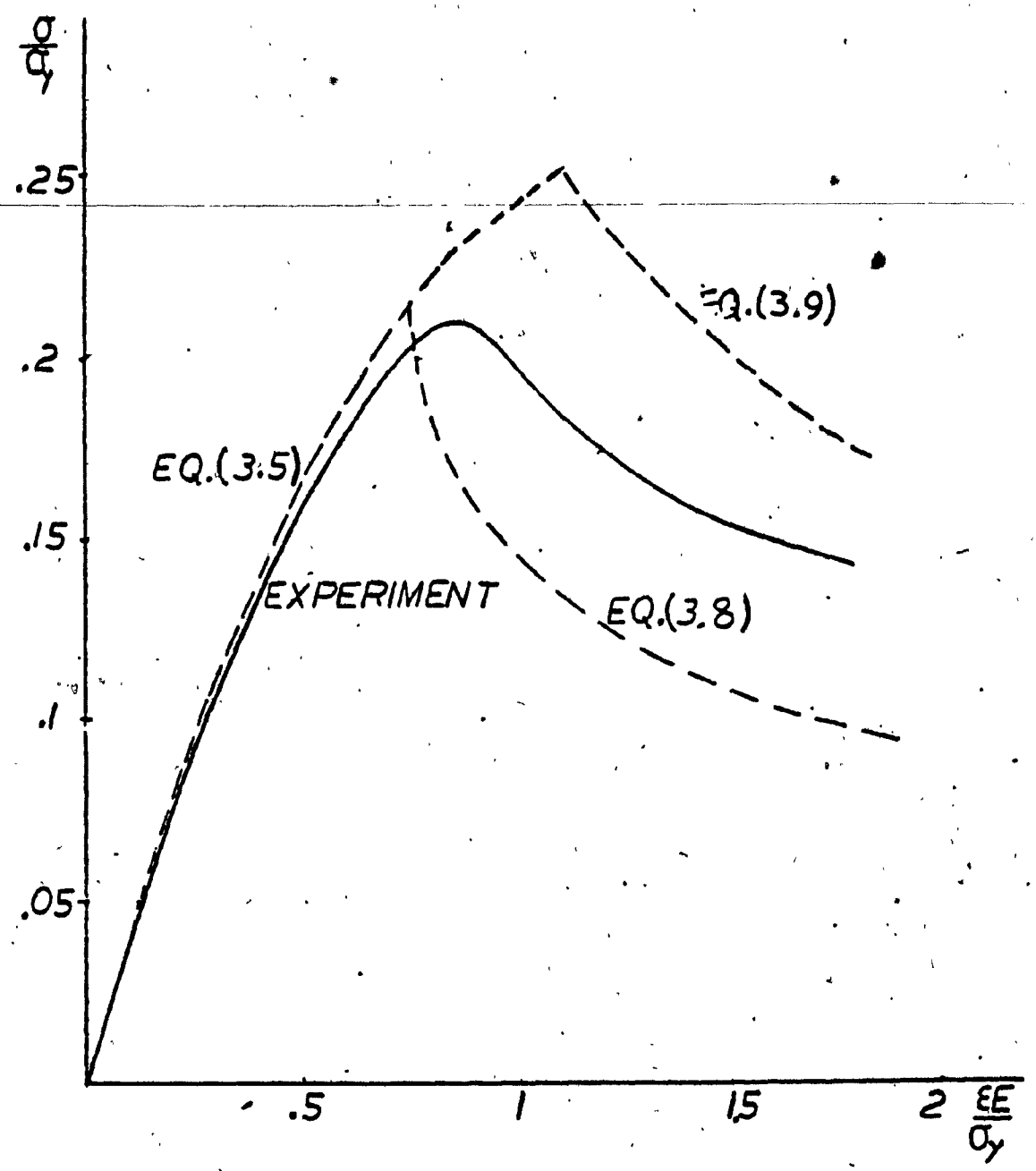

FIG. 4.5 LOAD-SHORTENING RELATIONSHIPS FOR T-SHAPE STRUTS (L/r =80)

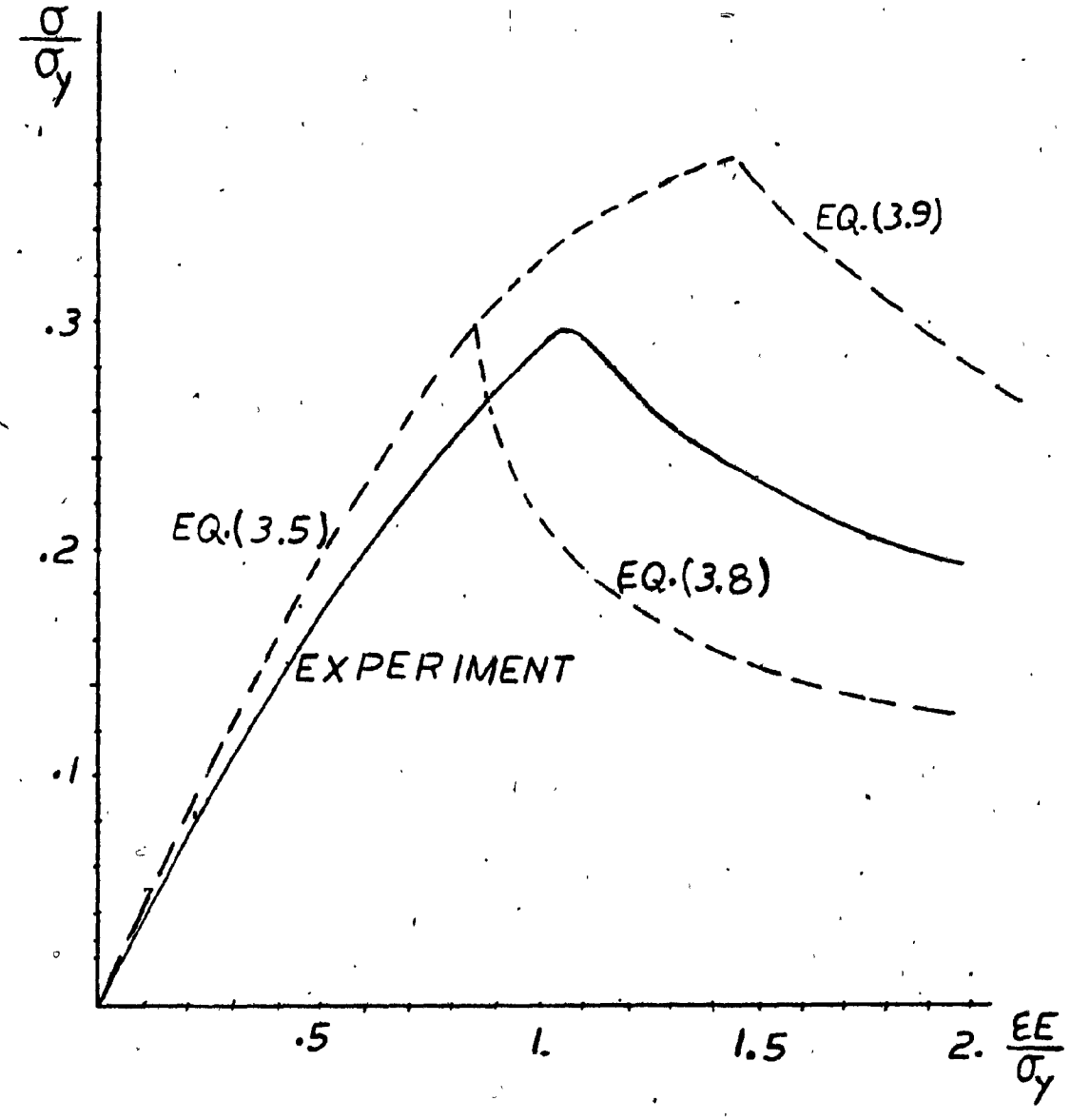

FIG. 4.6 LOAD-SHORTENING RELATIONSHIPS FOR T-SHAPE STRUTS (L/r =56)

II - Peak region of the loading-unloading curve.

In our experiments this region has a smooth crest. There is no sharp drop between phase I - III and as anticipated the crest is shorter for the less slender struts. The maximum capacity is close to that predicted using an elastic model up to first yield.

III - Unloading phase

The unloading curves from the experiment lay between the theoretical curves for extreme fibre yield (3-8) and a fully plastic stem (3-9) moving in general, toward the fully plastic model as shortening progressed. However, the important part in the present study is the elastic loading range up to the maximum capacity of the strut. The unloading region could be useful for computing the ultimate load capacity of the truss.

4.7 Equivalent Stiffness of Eccentrically Loaded Struts

For axially loaded struts the behaviour is linear and the axial stiffness is defined by $\frac{EA}{L}$. For eccentrically loaded strut the stiffness is no longer $\frac{EA}{L}$ and the load-shortening relationship is no longer linear as discussed in Chapter 3, and is given theoretically by equation (3.5).

For analytical purposes the theoretical relationship is approximated by two straight lines (Fig. 4.7).

The slope of a straight line is:

$$S = \frac{\sigma/\sigma_y}{\varepsilon E/\sigma_y} = \frac{\sigma}{\varepsilon E}$$

The slope S for concentrically loaded diagonal struts is unity (Hooke's Law). In eccentrically loaded diagonals the slope of a straight line, in load-shortening relationship diagram, is obtained by using an equivalent area (A'):

$$\delta = \frac{PL}{A'E} \quad \therefore \quad A' = \frac{PL}{\delta E} = \frac{\sigma}{\varepsilon E} A \quad \therefore \quad A' = SA$$

Thus the equivalent area for each of the two straight lines in Fig. (4.7) is equal to the gross area (A) times the slope of the load-shortening curve. The location of the point B1 is arbitrary, and is chosen so that the two straight lines reflect the curve as realistically as possible. Given y_1, the value of x_1 can be found from (3.5), and by knowing y_2, x_2 (the maximum capacity and corresponding shortening), the value of A_1 and A_2 are given by:

$$A_1 = \frac{y_1}{x_1} A \qquad (4.1)$$

$$A_2 = \frac{y_2 - y_1}{x_2 - x_2} A \qquad (4.2)$$

where A_1 and A_2 are equivalent areas of the eccentrically loaded strut in first and second stagesof loading behaviour.

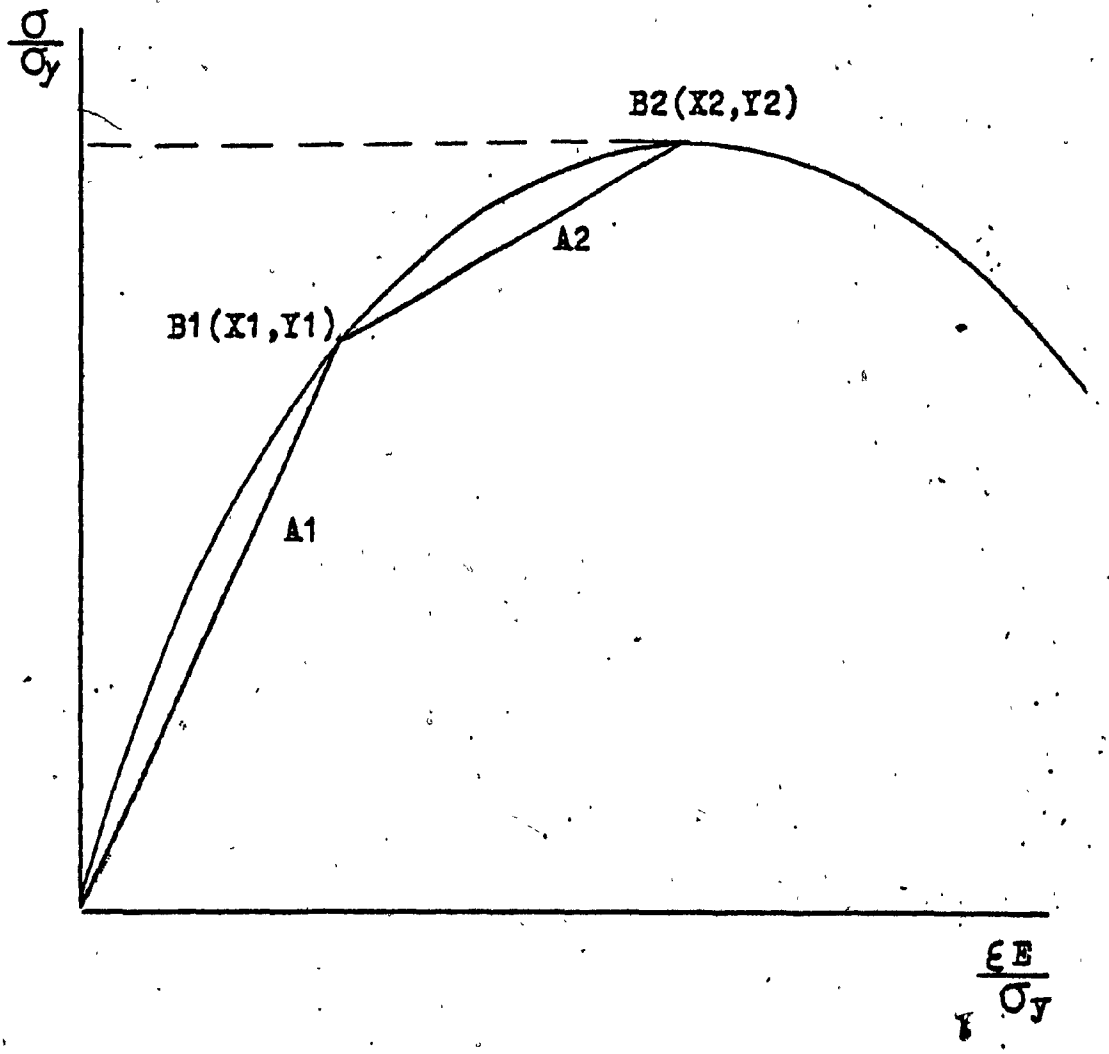

FIG. 4.7. GENERAL NON-LINEAR LOAD-SHORTENING RELATIONSHIP CURVE, ASSUMPTION OF TWO STRAIGHT LINESIN THE LOADING PHASE.

CHAPTER V

COMPUTER PROGRAM DESCRIPTION

5.1 INTRODUCTION

A computer program had been developed under the direction of Marsh [16] and used initially for the collapse analyse of orthogonal grid space trusses with concentrically loaded members. This program has been modified for analysing trusses with eccentrically loaded diagonals.

5.2 Computer Program Structure

The program performs a series of elastic analyses using the stiffness method. Three different approaches can be followed:

1) Elastic analysis: the first member which reaches its capacity in compression or tension limits the analysis (Fig. 5.1a).
2) Elastic plastic analysis: the buckled or yielded members become fully plastic and undergo plastic deformation without changes in their forces. (Fig. 5.1b)
3) Elastic unloading: the buckled members go into unloading phase which is introduced to the computer by using a negative area (Fig. 5.1c).

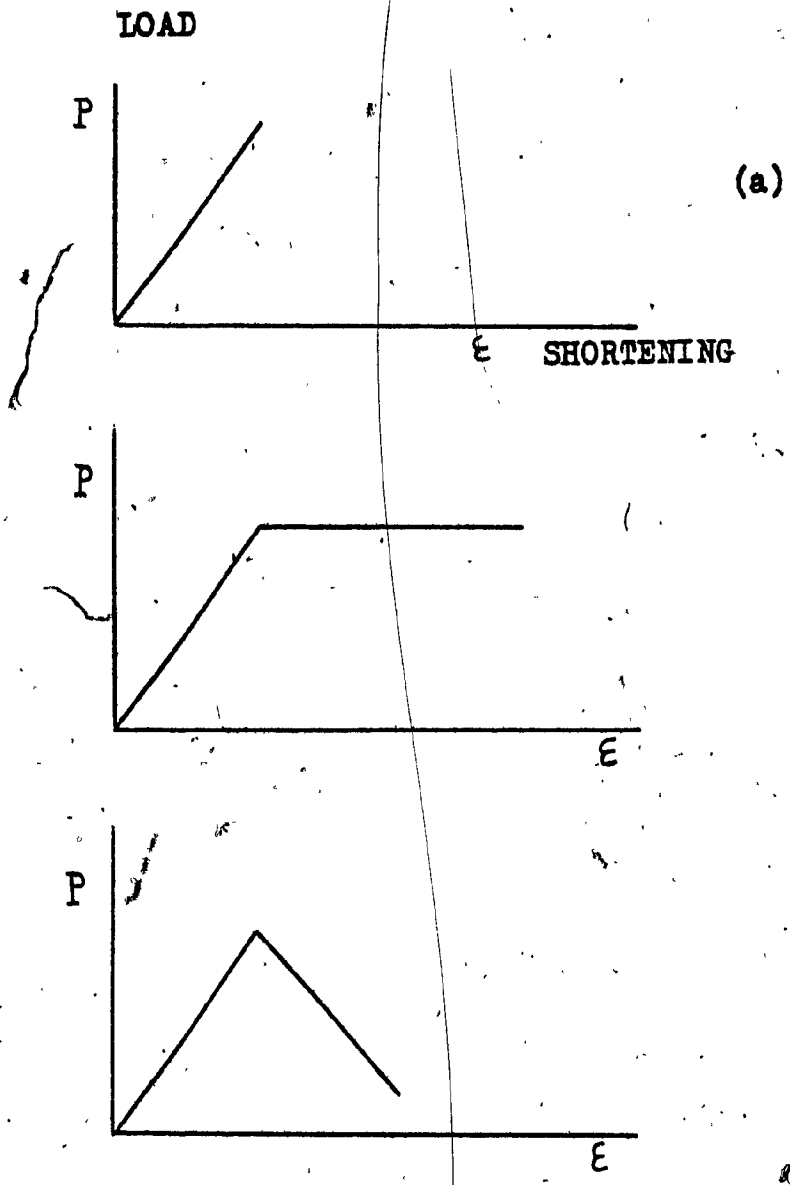

FIG. 5.1 LOAD-SHORTENING RELATIONSHIPS USED IN COMPUTER PROGRAM

a): ELASTIC BEHAVIOUR

b): ELASTIC-FULLY PLASTIC

c): ELASTIC-UNLOADING

The procedure in the computer program is similar to that used by Shin Be [23] for space trusses. The following steps are used for the analysis:

Step 1: The geometry of the truss: the numbers and size of the bays and depth of the truss are input.
Member properties: Area and capacities in tension and compression (P_t, P_c) and elastic modulus, E, are input.

Step 2: Elastic Analysis: A unit load is applied to all nodes. The displacement of the joints [X] are related to the elongations [x] of the members by:

$$[x] = [c] \cdot [X] \tag{5.1}$$

Matrix [c] is called the kinematics matrix. Forces in the members [P] are found from the load-elongation relationship.

$$P = \frac{EA}{L} x \tag{5.2}$$

This is expressed in matrix form by:

$$[P] = [S] [x] \tag{5.3}$$

[S] is the member stiffness matrix, [P] is the internal force matrix. [W], the external joint loads, should be in equilibrium with internal forces [P] if the structure is stable;

$$[W] = [A]\,[P] \tag{5.4}$$

in which the matrix [A], called the static matrix, is the transpose of [c].

$$[A] = [c]^T \quad \text{or} \quad [c] = [A]^T \tag{5.5}$$

From (5.4) and (5.5) we have

$$[W] = [A] \cdot [S]\,[A]^T \cdot [X] \tag{5.6}$$

[A] and [S] can be determined according to the geometry of the structure and to the types and sizes of the members. [W] is given.

From (5.6) matrix [X] is obtained and from (5.1) matrix [x] is calculated. Using (5.1), (5.3) and (5.5) we get:

$$[P] = [S] \cdot [A]^T \cdot [X] \tag{5.7}$$

Step 3: Calculation of Force Factors:

The capacity of each member (P_t or P_c) is divided by the force in the member, [P_1], due to the unit load. The resulting ratios are force factors. The smallest of these force factors is called K_1.

Step 4: Residual Capacities:

The forces in all members $[P_1]$ are multiplied by the ratio K_1, to give matrix $[K_1P_1]$. To find the residual force in each member, the forces $[K_1P_1]$ are subtracted from the members' capacities (P_t or P_c), leaving the residual capacities, $(P_t-K_1P_1)$ or $(P_c-K_1P_1)$.

Step 5:

Those members that are left with zero capacity (or less than a selected small amount) are removed from the structure. The failed members are replaced either by the plastic or the unloading condition simply by changing their area to zero or a negative number, respectively.

Step 6:

The new capacities of the members are the residual capacities $(P_t-K_1P_1)$ or $(P_c-K_1P_1)$. (It is to be noted that compression force in a member will reduce the compressive capacity and increase the tensile capacity. This consideration covers those cases where load reversals occur as yielding progresses).

The converted truss (with residual members' capacities) is re-analysed for unit load by repeating steps (2) to (5). The new force factor K_2 will be obtained and more members, whose capacities are exhausted, are replaced by zero or negative area.

In any cycle some members are removed from the truss. This procedure continues until either the stiffness matrix becomes singular, i.e. the structure is not stable; or, where negative areas are used, the load increment becomes zero at the limiting capacity due to the internal equilibrium reached between the forces in the members. The ultimate load capacity of the truss is the sum of the force factors (K).

The displacements of joints and elongations of members are also given in the output of the computer program.

5.3 The Modified Computer Program for Eccentrically Loaded Diagonal Space Trusses

As already discussed in Chapter 3, the behaviour of struts under eccentric load is non-linear (Fig. 4.7).

In concentrically loaded diagonals the pair (P_c, A) is the property of each member. In eccentrically loaded member the pairs (P_{c1},A_1), (P_{c2},A_2) are required. The computer program is modified to accept this piece-wise behaviour for diagonals through the following procedures:

- Properties of chords are the same as in the original program, but for diagonals (P_{c1}, A_1) is the capacity and area.

- A unit load is applied and forces in all members are computed.
- The diagonals which reach the first part of their capacities (P_{c1}) are then replaced by (P_{c2}, A_2).
- The other members which have not reached their first capacities are replaced by their residual capacities.
- The procedure continues and each time a member reaches the end of the first stage of its capacity, it is replaced by area (A_2) and its residual capacity. When the first diagonal reaches point (B_2) where its entire capacity is exhausted (Fig. 4.7), it may be given a negative area, as discussed in section (5.2) step 5, to find the truss' ultimate capacity. (The reserve beyond the point when the most highly loaded diagonal reaches its limiting capacity has been found to be small).
- The other procedures are exactly like those of the original program, explained in the previous section (5.2).

CHAPTER VI

INFLUENCE OF ECCENTRICALLY LOADED DIAGONALS ON THE BEHAVIOUR OF SPACE TRUSSES

6.1 INTRODUCTION

Generally when the chords control, because they behave as if concentrically loaded, failure of the truss is brittle. Diagonals, when concentrically loaded, also buckle suddenly, but as they are separate pieces and discontinuous, they may be loaded eccentrically. As discussed in Chapter 3, the eccentricity gives a non-linear behaviour and gradual bowing prior to reaching their maximum capacities. The influence of T-shape diagonals on the behaviour of triangulated space grids is the subject of this chapter.

When the T-shape diagonals control the collapse load two phenomena are observed:

1) The bow in the diagonals increases gradually and becomes noticeable prior to attaining the maximum capacity. Because there is no sudden buckling, the distribution of interior forces changes smoothly, and the truss behaves in a "quasi ductile" manner. This gradual bowing provides a visible sign of distress, which could give enough time to evacuate the building.

2) The axial stiffness of the T-shape diagonals decreases with increasing load. As the diagonals control the force carried by the associated chords, this allows the transfer of force to other chords.

The influence of T-shape diagonals on the truss varies depending on the support locations. The two most commonly used types of support arrangement are four-corner, and boundary. For each type, two trusses were analysed; one with eccentrically loaded diagonals, the other with concentrically loaded diagonals, and the results were compared.

6.2 Four Corner Supported Orthogonal Grid Space Truss with T-Shape Diagonals

A truss composed of 12x12 bays and supported on four corners (fig. 6.1) was analysed with both concentrically and eccentrically loaded diagonals. The design was such that diagonals always controlled, achieved simply by using chords strong enough not to buckle or yield. All the chords were assumed to be equal in size and capacity, as were the diagonals (table 6.1). The change from the first to the second stage of loading, for diagonals, was at 0.8 of the ultimate capacity of struts (Fig. 6.2).

Member Type		Area mm^2	P_t KN	P_c KN
Chords		1000	100	50
Diagonals concentrically loaded		300	50	15
diagonals eccentrically loaded	1st part	80	40	12
	2nd part	30		3

Table 6.1

Properties of Chords and Diagonals used for Analyses of Trusses

Forces in the chords for both concentrically and eccentrically loaded diagonals from computer analysis of the 12x12 bay truss is shown in Figure (6.3). As seen in Table 6.2, the capacity of the truss for both kinds of diagonal is equal while the required chord capacity decreased almost 12%. This decrease is due to more uniform distribution of forces in the edge chords.

Diagonal Type	Max. truss capacity per node KN	Chord Capacity KN	Diagonal force KN
Concent. loaded	0.32	37	15
Eccent. loaded	0.32	33	15

Table 6.2

Computer Result for Truss and Chord Capacities.Four Corner Supported

The stiffness of the T-shape diagonal $\overline{AC}$ (Fig. 6.3) decreases with increasing load, causing less load to be transfered to the edge chord, as $\overline{AB}$ accepts and transfers more load to the second chord giving a more uniform force distribution between the chords.

The chords in the central region carry almost the same force for both eccentrically and concentrically loaded diagonals.

6.3 Boundary - Supported Trusses

A truss identical to the one discussed in section (6.2), with the same member properties shown in Table 6.1, but supported along the boundaries under uniform load, was analysed. Again the diagonals reached their maximum capacities first. Referring to Fig. (6.4) for concentrically-loaded diagonals, the central boundary diagonal ($\overline{AD}$) reached its maximum capacity first. The forces in the other diagonals

and chords are shown in Fig. (6.4). In the case of T-shape diagonals, the same diagonal, $\overline{AD}$ (Fig. 6.4), was the first to reach its first stage of capacity (Fig. 6.2). On increasing the applied load the diagonal $\overline{AD}$, possessing less stiffness, accepts less load. Consequently, the other diagonals along the edge, progressively from the middle toward the corners, accept more load until they also pass their first stage of loading. Finally, the first diagonal ($\overline{AD}$) reaches its maximum capacity. The analysis for the 12x12 bay truss required 10 cycles, each showing that a diagonal reached its first stage of capacity.

The forces in the diagonals and chords, when diagonal $\overline{AD}$ reached its maximum capacity, are shown in Fig. (6.4). As is seen, the forces in the chords are very close. The computer output showed a 4% increase in capacity for the eccentrically loaded diagonal truss compared to the concentrically loaded one (Table 6.4).

Diagonal Type	Max. truss capacity per node KN	Chord capacity kN	Diagonal force kN	
Concent. loaded	2.176	96.4	15	
eccent. loaded	2.276	95	15	First stage 1 2 second stage 3

Table 6.3 - Computer Result for Boundary - Supported Truss

Although the increase in load carrying capacity of the truss is not great, the important effect of T-shape diagonals in boundary-supported trusses is the resulting "quasi-ductibility". A more uniform distribution of the shear forces along the boundaries, in comparison to the truss with concentrically loaded members, was also achieved.

6.4 Optimization

Marsh, in his paper [21] discusses optimization based on heavier chords towards the edges which have a total capacity equal to that of the chords in the central zone. Again, a 12x12 bay, four corner supported truss was modeled to analyse for optimization. The arrangement of heavy and light chords is shown in Fig. 6.5 and Table 8.5.

Member type		Area mm^2	P_t KN	P_c KN
Heavy chords		960	60	45
Light chords		480	35	25
Concent. diagonals		300	50	15
Ecc. diagonals	1st stage	80	30	12
	2nd stage	30		3

Table 6.4 - Member Properties for Optimum Truss

The analysis shows a 20% increase in load carrying capacity for a truss with T-shape diagonals over that with concentrically loaded diagonals. The forces in the chords are shown in Fig. 6.5. The T-shape diagonal truss has better moment distribution between the boundary zone chords, and most of the chord capacity has been used.

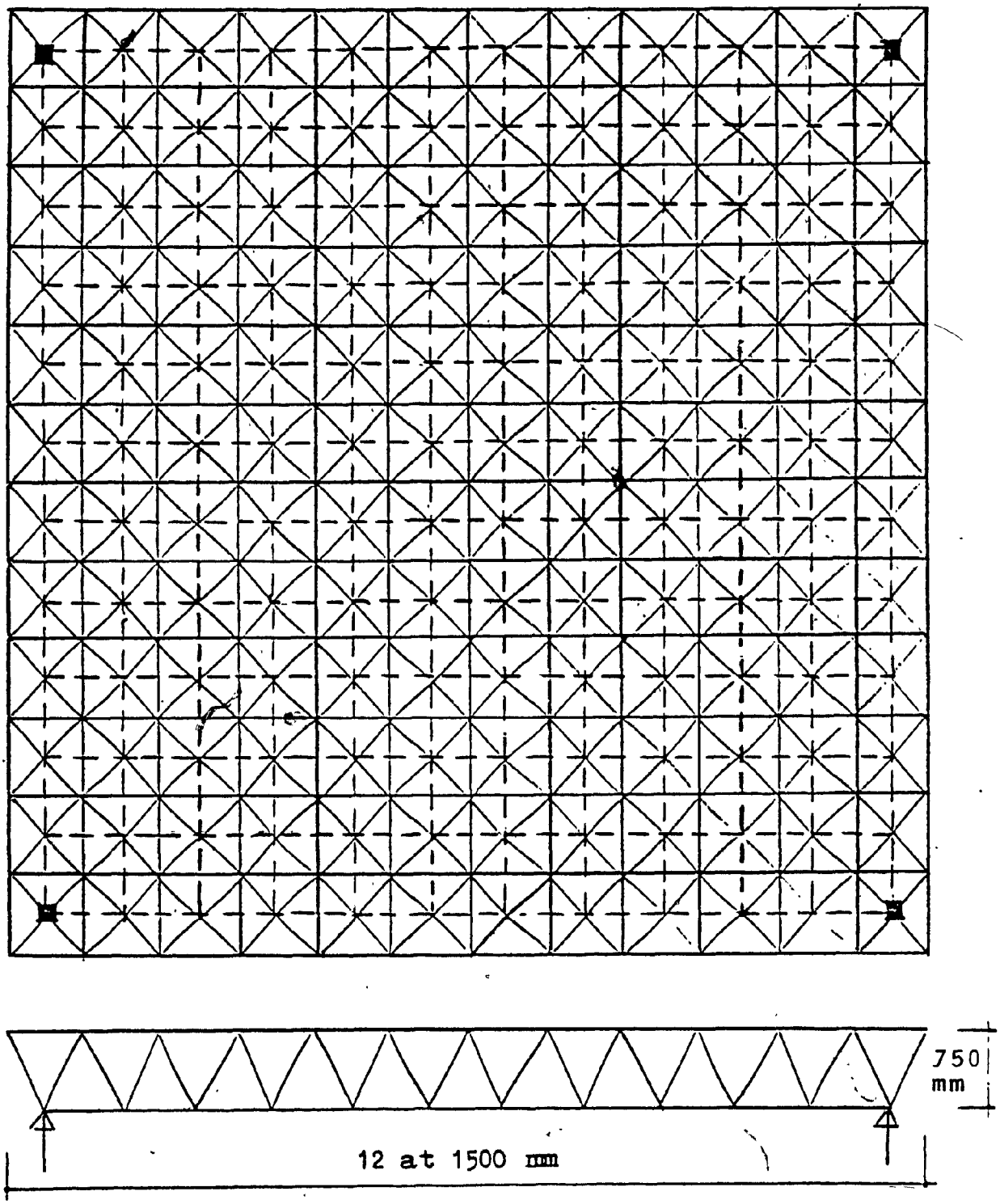

FIG. 6.1 A12×12 BAY FOUR CORNER SUPPORTED ORTHOGONAL GRID SPACE TRUSS

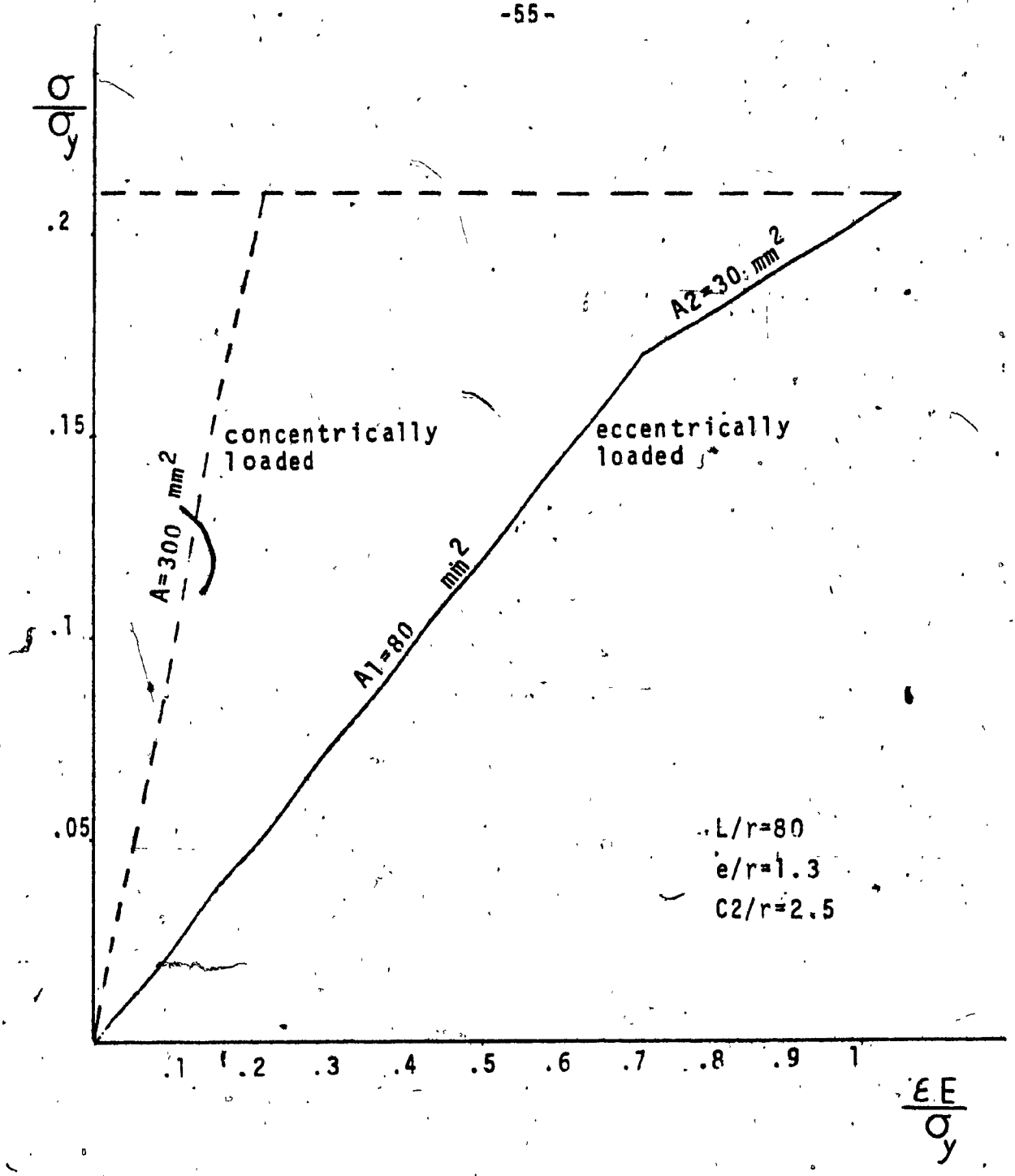

FIG. 6.2 EQUIVALENT AREA FOR AN ASSUMED T-SHAPE STRUT USED IN ANALYSES

Forces in diagonals (kN)

	AC	AB	DE	GF	JH	KL	MN
Ecc	-1.5	-1.38	-.77	-.46	-.21	-.14	-.03
Con	-1.3	-1.5	-.91	-.55	-.32	-.16	-.03

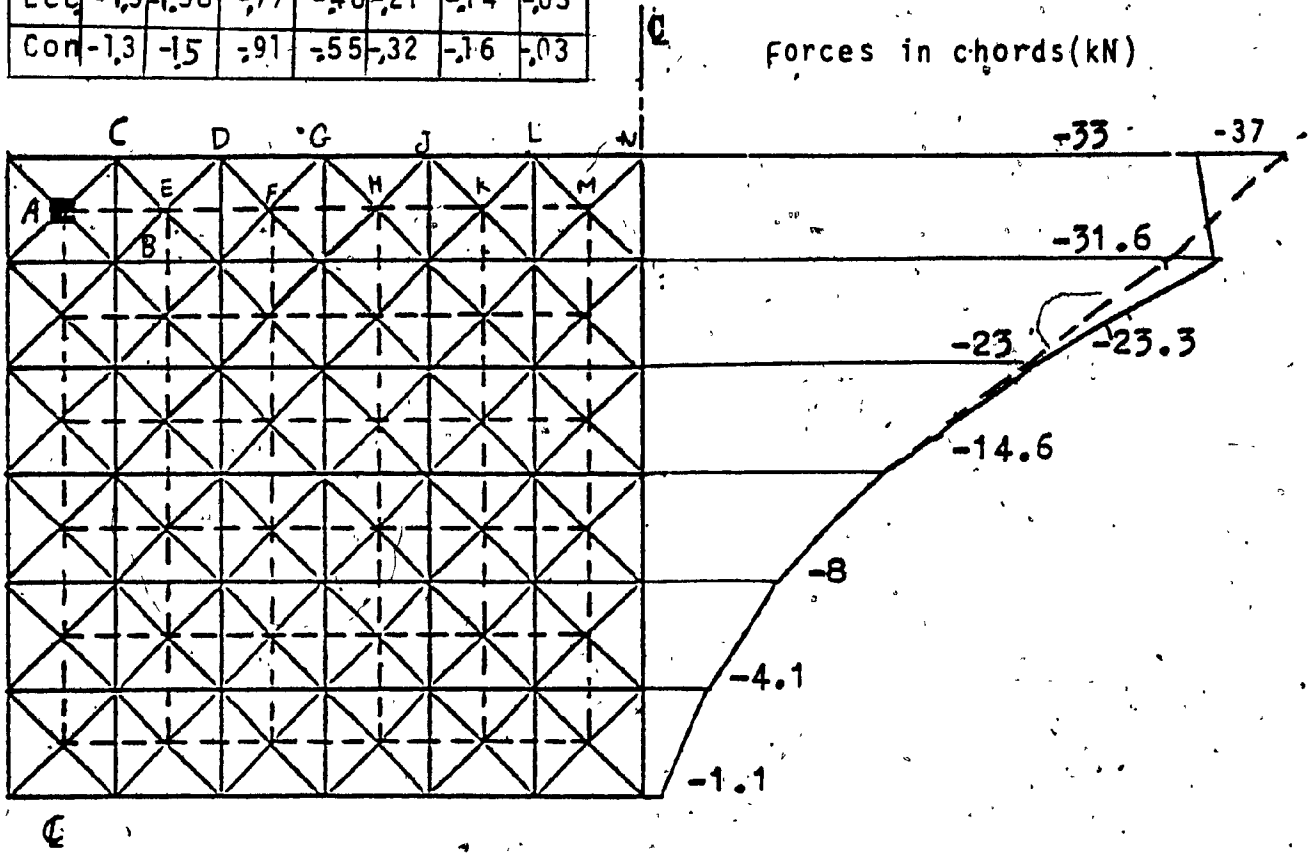

——— ECCENTRICALLY LOADED DIAGONALS

– – – – – CONCENTRICALLY LOADED DIAGONALS

FIG. 6.3 FORCES IN CHORDS AND DIAGONALS

FOUR CORNER SUPPORTED TRUSS WITH UNIFORM CHORDS

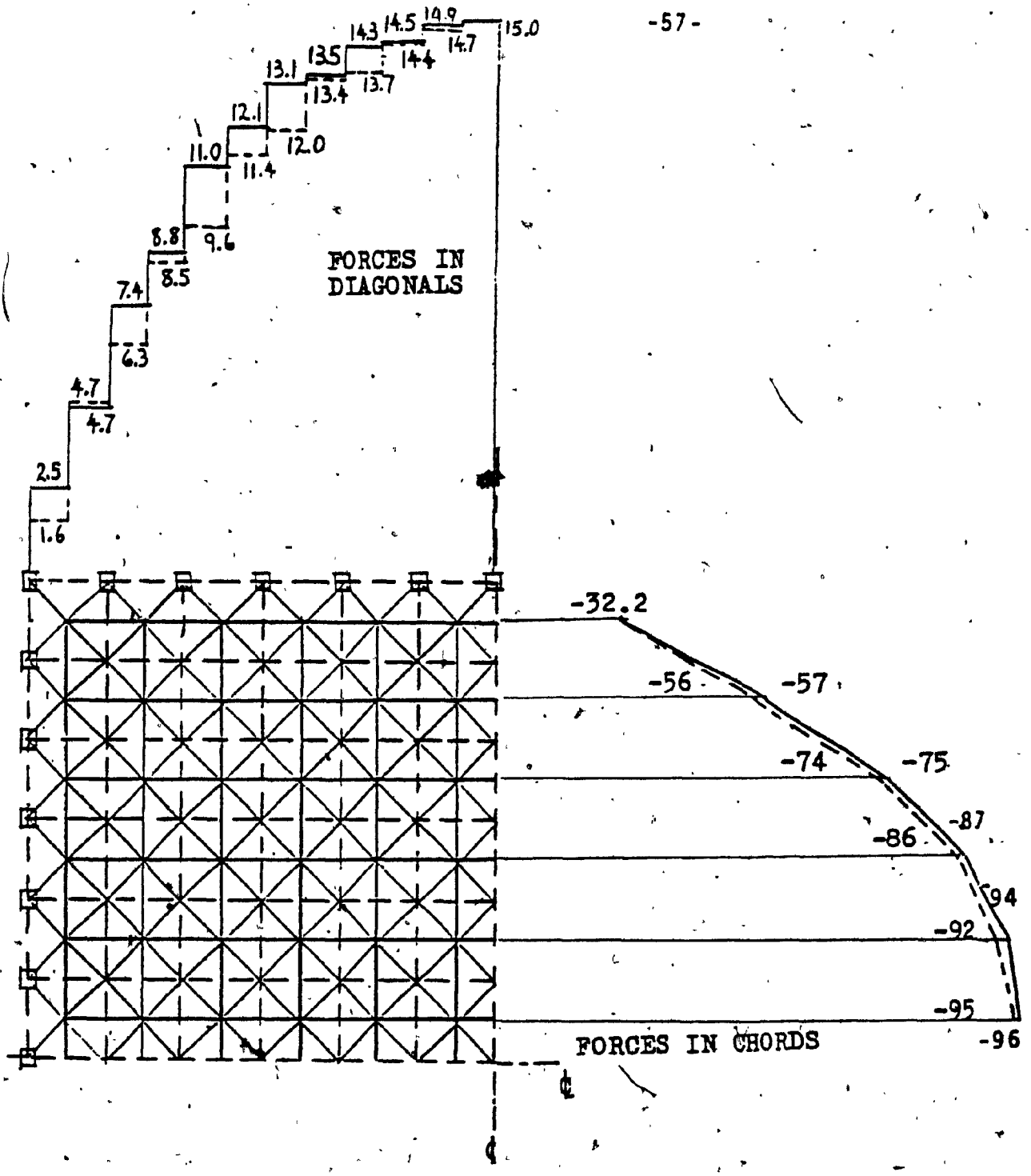

FIG. 6.4 FORCES IN THE DIAGONALS AND CHORDS (kN)
BOUNDARY SUPPORTED TRUSS,

Forces in Diagonals

	AC	AB	DE	GF	JH	LK	NM	Capacity of truss
Con.	15	11.1	9.7	6.1	3.6	1.7	0.3	0.306
Ecc.	14.7	15	8.7	5.3	3.1	1.5	0.3	0.337

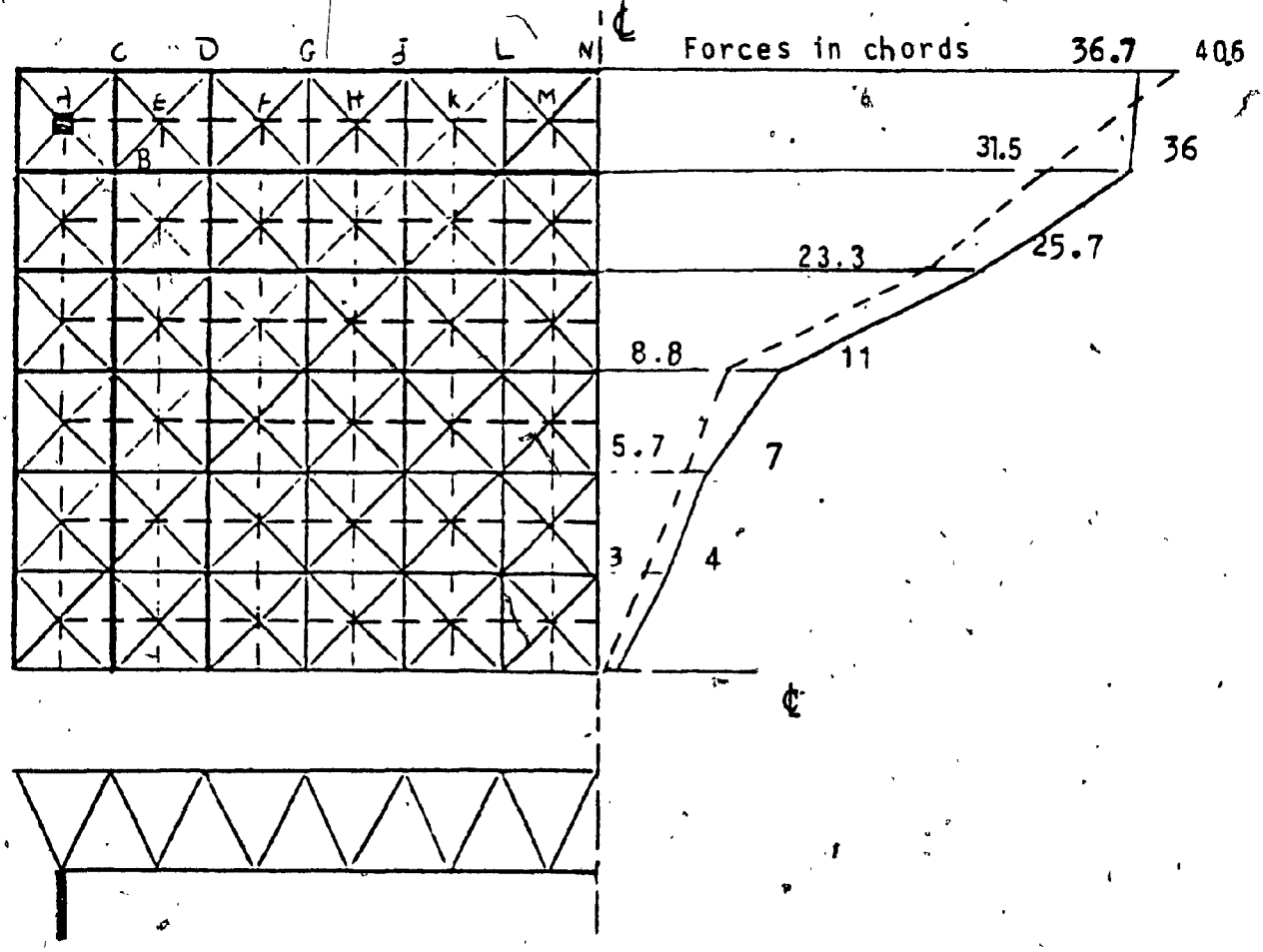

——— ECCENTRICALLY LOADED DIAGONALS

- - - - - - CONCENTRICALLY LOADED DIAGONALS

FIG. 8.5 FORCES IN A TRUSS WITH HEAVIER BOUNDARY ZONE CHORDS

CHAPTER VII

TEST ON SPACE TRUSS

7.1 INTRODUCTION

In order to show the principles of the influence of T-shape diagonals on the behaviour of space trusses, and to compare theory to experiment, a small 3x2 bay space truss was tested. The truss was designed so that the middle chord (4-14) would approximately take twice as much load as the side chords (3-13, and 5-15), if the diagonals were concentrically loaded (Fig. 7.1). By using T-shape diagonals, as the load increases, the stiffness of central diagonals decreases, and transfer less load to the middle chord. The result is that, as the ultimate capacity is approached, all chords carry almost equal load.

7.2 Description of the Test Model

The truss was composed of 2x3 equal 1316 mm bays, and was 658 mm high. The chords were 50.8 x 50.8 x 3.17 mm steel angles. The maximum capacity in tension was calculated based on gross area, from which the area of the two holes was subtracted. The maximum tensile and compressive capacity for chords are given in table 7.1.

Chords	Area mm^2	L/r	P_t KN	P_c KN
Steel angle	300	130	36	35

TABLE 7.1 - Test Chords Properties

Diagonals were T-shape aluminum alloy (Fig. 7.2) with the properties as follows:

$A = 400 \ mm^2$

$r = 11.2$ mm

$L = 1100.$ mm (centre to centre of the holes)

$\frac{L}{r} = 98$

$\sigma_y = 230 \ MP_a, = 73.4 \ MP_a$

$C_1/r = 0.9$, $C_2/w = 2.5$

$\frac{e}{r} \simeq 1.1$ assuming application of load at the middle of the flange of the attached angle, 3.2 thick (Fig. 9.2).

Using the theoretical relationships (3.5) and (4.1, 4.2), the capacities and shortening of the first and second stage were chosen such that the end of the first stage was at approximately 0.75 of the ultimate capacity. This ratio was obtained from trial analyses and gave the most uniform distribution of load in the chords.

$y1 = 0.13$, $x1 = 0.43$, $y2 = 0.18$, $x2 = 0.93$

By using relation (4.1, 4.2), the equivalent areas of each stage of non-linear loading of T-shape diagonals are found (Table 7.2).

Diagonals		Area mm^2	P_t kN	P_c kN
Corcentrically loaded		400.	70.	16.5
Eccentrically loaded	1st stage	120	54.	12
	2nd stage	40	16.	4.5

TABLE 7.2 - Properties of the Test Diagonals

7.3 Load and Deformation Measurements

Loading: The loading system was composed of three jacks, installed on joints, 4, 9, 14 (Fig. 7.1), by which compressive loads were applied. Special connections were made for the tips of the jacks to transfer the forces to the angles in the joints. The truss was fixed to a bed by four square rods. Readings of the loads were taken from separate gauges on each of the jacks.

Strain: Two gauges were mounted on each chord, one on each side of the neutral axis of the section. At each load increment, the strains in the three compression chords were measured. Fig. 7.1 shows the locations of the strain gauges.

Deflection: Four dial gauges were used to measure the vertical movements of the nodes 4, 9, 3, 8 (Fig. 7.1). The maximum deflection was expected to be at central joint 9, therefore only deflection of point 9 is shown in Fig. 7.7.

7.4 Test Procedure

The loads on the three nodes (4,9,11) were simultaneously increased in increment of 1800 KN. After each increment of load, readings were

taken for load, strain, and deflection. Also the bows in diagonals were observed, and pictures were taken.

The loads were increased until the strains in the chords were almost equal to each other. The loads were then removed. The diagonals became straight again, and the measured residual strain was negligible. This means that the system was in the elastic range.

7.5 Test Results

The load on the three nodes (4,9,14) when the middle and side chords carried equal forces was 21600 kN. Table 7.1 show the strain in central chord and the average strain in the side chords.

The area of each chord is 300 mm^2. The modulus of elasticity for steel is 210 GPa, and 70 GPa for aluminum. The forces, F, in the chords were computed from Hooke's law, $F = E \varepsilon A$. For each applied load, corresponding chord forces are shown in Table 7.2. These are plotted in Fig. 7.3.

Diagonal forces: From the condition of equilibrium in Fig. 7.4, if the forces in the edge or middle chords are given, all the forces in the other chords and diagonals can be calculated.

The forces in the diagonals 1-4 and 1-3, (Fig. 7.4), obtained from equilibrium, are listed in Table 7.4 and plotted in Fig. 7.5.

One of the most important results of the test was the observation of the bow of the diagonals. Before applying the load, the diagonals were all straight to the eye. On applying the load the diagonals started to bow. When the load on each node was 17100 kN the deflection at the centre of the diagonal 1-4 (Fig. 7.1), with the length of 1100 mm, was 9 mm, and at 21600 kN was 20 mm. The bowing was gradual and noticeable.

Deflection: The deflection of the central point (9) of the truss (Fig. 7.1) was measured in the experiment and plotted vs. applied load in Fig. 7.6. Also plotted in the same figure is the computer analysis result for a truss with concentrically loaded diagonals.

7.6 Discussion of the Test Results

The following points were considered:

- The results from computer analysis are limited to the point where the first diagonal reaches its maximum capacity.
- The weight of the structure was negligible.
- Although the truss was symmetrical and the three loads equal, because the loads were applied and controlled manually, and due to built-in imperfections in the structure, some differences were measured in force for two similar chords which, theoretically, should carry identical loads.

- The maximum capacity of the truss in the experiment was 21600 KN. This value was used as the maximum applied load in the computer analysis for trusses with both concentrically and eccentrically loaded diagonal.

Comparison between forces which were carried by the middle and side chords shows a good agreement between experiment and theory. (Fig. 7.2). The ratio of the forces in the middle and side chords, when diagonals are loaded concentrically (Table 7.4), is 1.87. The ratio of the forces in chords, when diagonals are eccentrically loaded, is 1.1 experimentally and 1.25 theoretically. The difference between two ratios (1.87 and 1.10) shows that truss with eccentrically loaded diagonals has more uniform force distribution between chords than concentrically loaded one.

The ratio of the forces carried by the diagonals (1-3 and 1-4) was 1.87 according to computer results of concentrically loaded diagonals, and 1.31 experimentally for eccentrically loaded diagonals (Table 7.4). These two ratios show the improvement effected by allowing diagonal (1-4) to accept and transfer more load, which causes more even distribution in the chord forces.

An additional, but incidental finding was the deflection of the truss in the central point 9 (Fig. 7.1). The deflection of the

eccentrically loaded diagonal truss is more than that of the concentrically loaded one, which should be considered in truss design. The deflection for the truss with eccentrically loaded diagonals in the experiment was 20% more than the computer analysis for concentrically loaded diagonals. (Fig. 7.6).

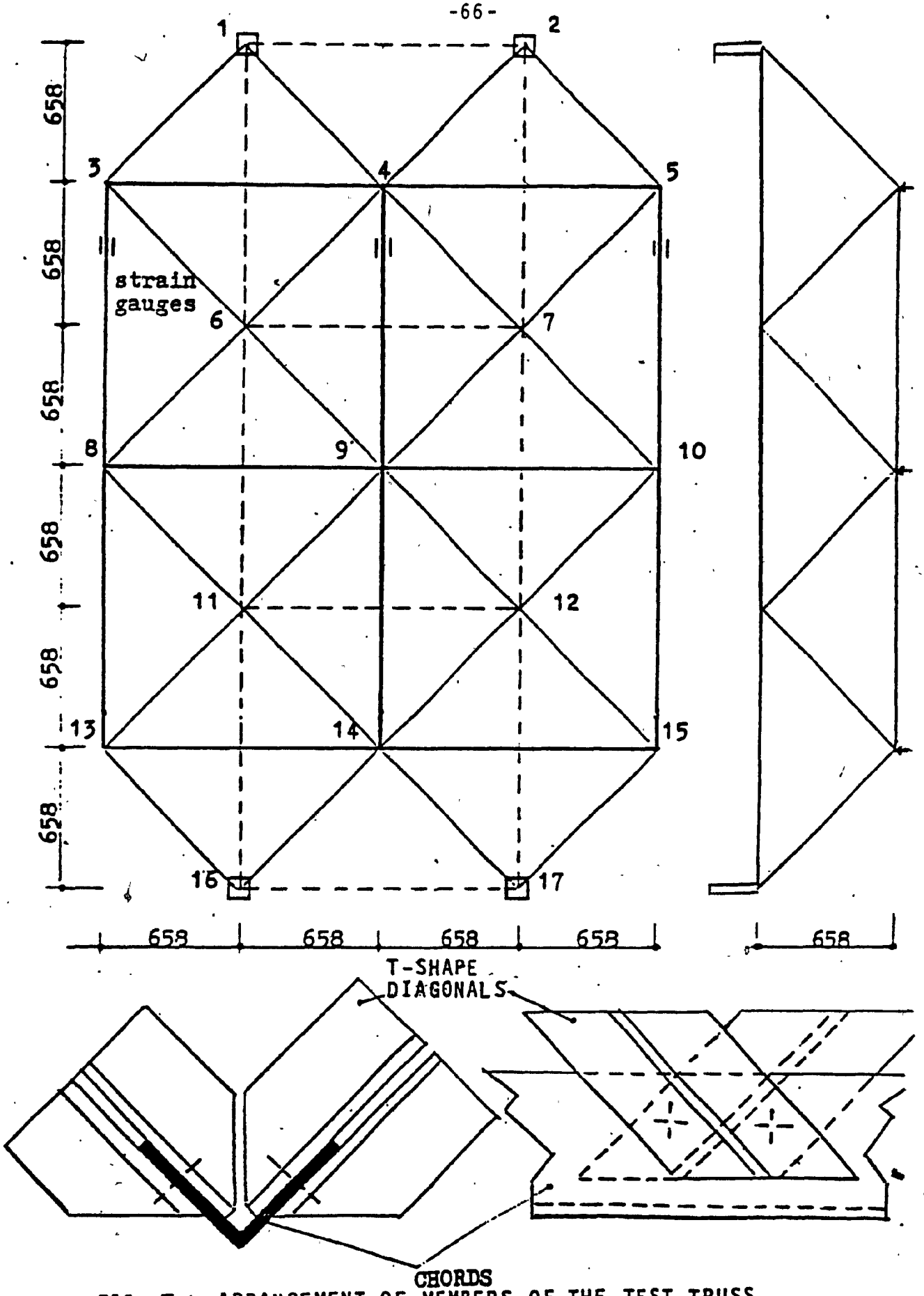

FIG. 7.1 ARRANGEMENT OF MEMBERS OF THE TEST TRUSS

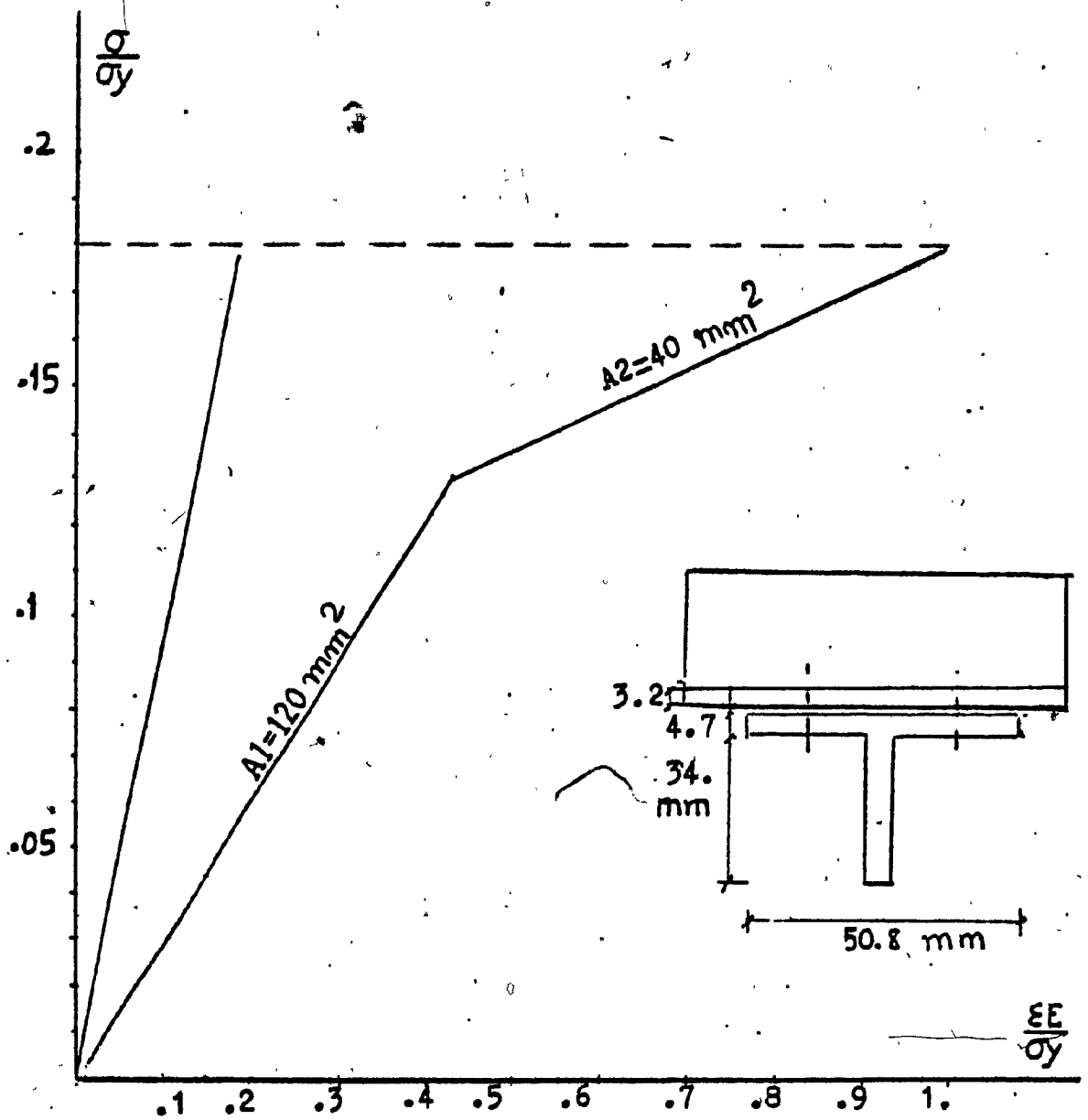

FIG. 7.2 EQUIVALENT AREA FOR T-SHAPE STRUT USED IN TEST TRUSS

Load on each node KN	Strain in Left Side Chord	Strain in Right Side Chord	Strain Average of side chord	Strain in in Middle Chord
1.8	13	15	14	27
3.6	27	29	28.5	54
5.4	43	46	44.5	80
6.3	52	56	54	92
7.2	58	62	60	103
8.1	70	73	71.4	114
9.0	78	81	79.5	125
9.9	88	90	89	137
10.8	97	99	98.5	148
11.7	105	107	106	157
12.6	113	115	114	167
13.5	124	128	125	176
14.4	134	136	135	185
15.3	144	146	145	195
16.2	153	155	154	205
17.1	164	166	165	214
18.0	174	176	175	222
18.9	183	185	184	230
19.8	194	196	195	237
20.7	207	209	208	243
21.6	223	225	224	248

Table 7.1

Applied Load and Strain in Chords from test

Load on Each Node kN	Forces in Side Chord kN	Forces in Middle Chord kN
1.8	.9	1.7
3.6	1.8	3.4
5.4	2.8	5.1
6.3	3.4	5.8
7.2	3.8	6.5
8.1	4.5	7.2
9.0	5.0	7.9
9.9	5.6	8.6
10.8	6.2	9.3
11.7	6.7	9.9
12.6	7.2	10.5
13.5	7.9	11.1
14.4	8.5	11.7
15.3	9.1	12.3
16.2	9.7	12.9
17.1	10.4	13.5
18.0	11.0	14.0
18.9	11.6	14.5
19.8	12.3	14.9
20.7	13.1	15.3
21.6	14.1	15.6

Table 7.2

Applied Load, Forces in Chords Obtained from Experiment

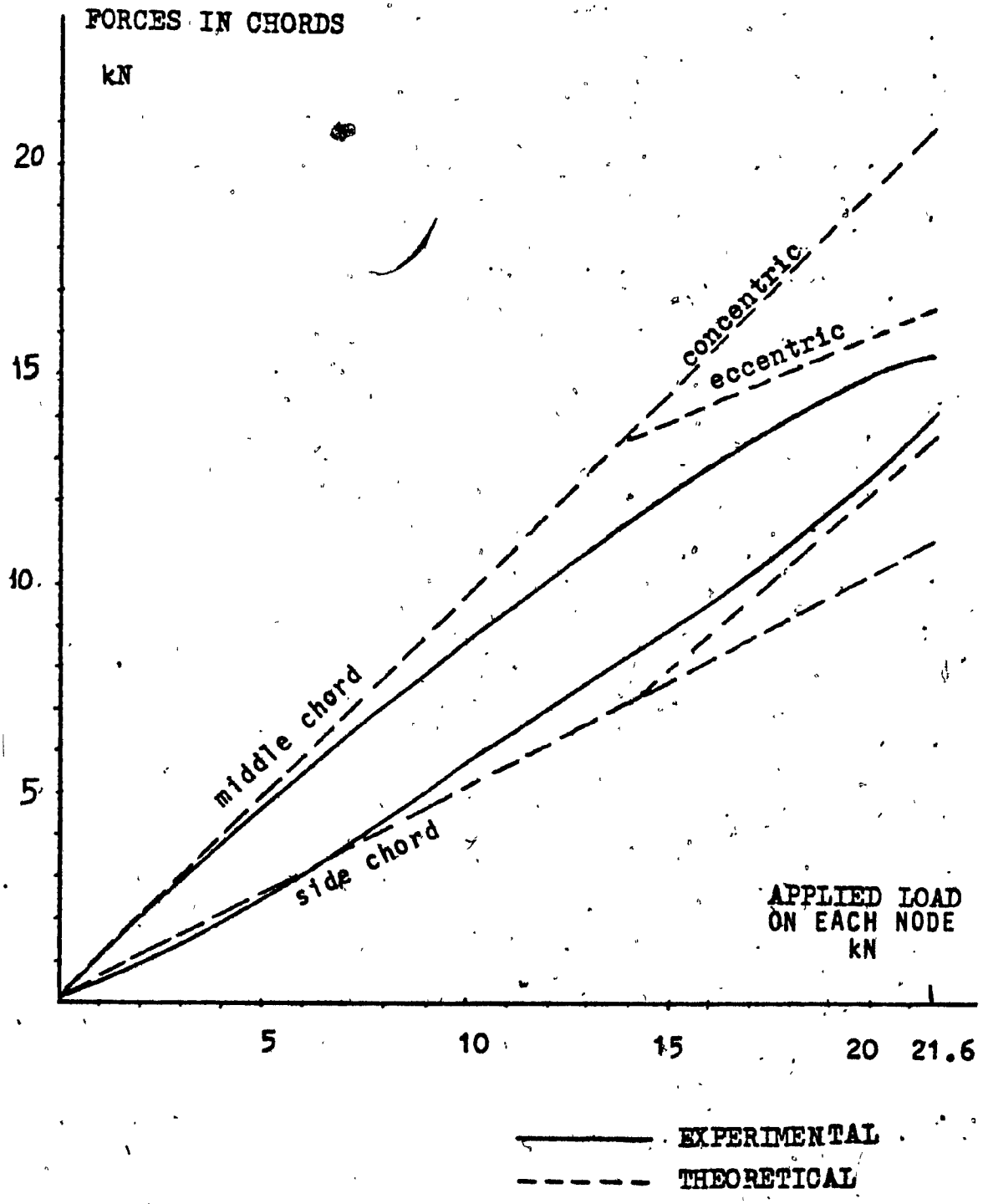

FIG 7.3 CHORD LOADS

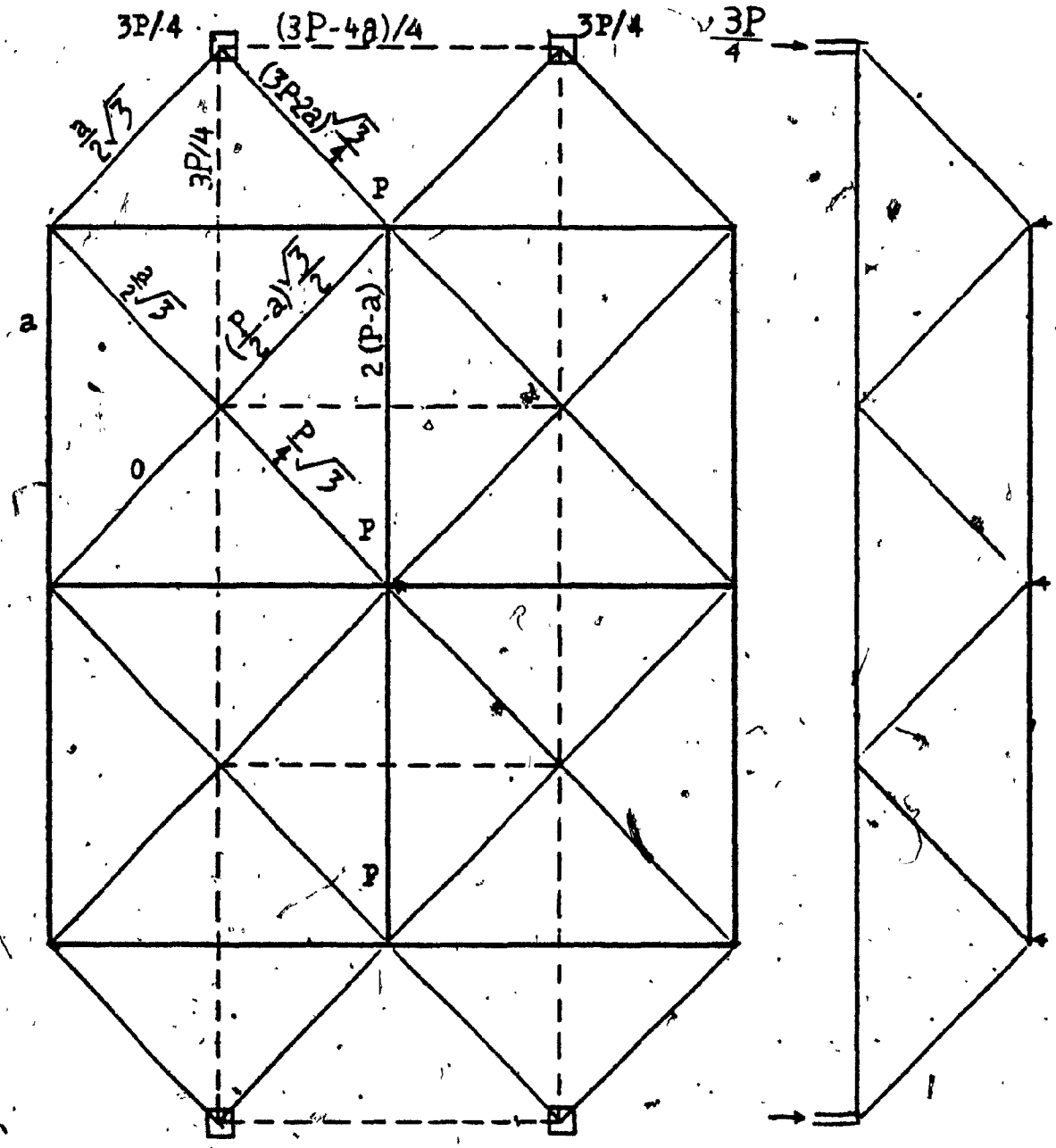

a: chord force from table 9.2
P: corresponding applied load

FIG. 7.4EQUILIBRIUM FORCES IN THE TEST TRUSS

Applied load on each node KN	Forces in diagonal (1 - 3) KN	Forces in diagonal (1 - 4) KN
1.8	0.78	1.56
3.6	1.56	3.12
5.4	2.42	4.59
6.3	2.94	5.24
7.2	3.29	6.06
8.1	3.90	6.62
9.0	4.33	7.36
9.9	4.85	8.01
10.8	5.37	8.66
11.7	5.80	9.40
12.6	6.23	10.14
13.5	6.84	10.70
14.4	7.36	11.35
15.3	7.88	12.00
16.2	8.4	12.64
17.1	9.00	13.21
18.0	9.52	13.86
18.9	10.05	14.50
19.8	10.65	15.07
20.7	11.34	15.55
21.6	12.12	15.94

Table 7.3

Forces in Diagonals Found from Equilibrium

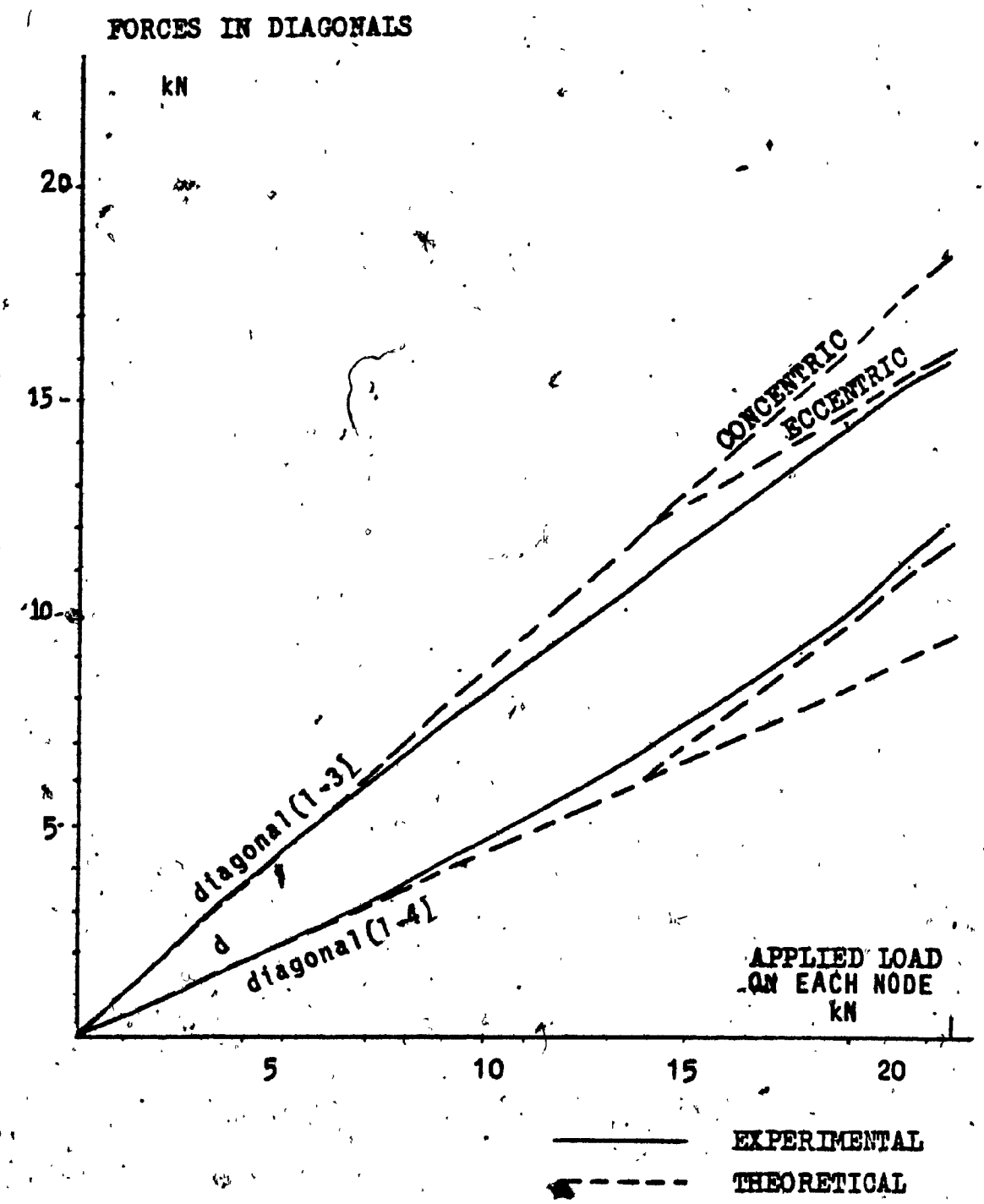

FIG. 7.5 DIAGONAL FORCES IN TEST TRUSS

FORCES IN MEMBERS kN

Applied on Each Node Load kN	THEORY				EXPERIMENT			
	Chords		Diagonals		Chords		Diagonals	
	Edge	Central	1-3	1-4	Edge	Central	1-3	1-4
5400.	2.9	5.4	2.4	4.5	2.8	5.1	2.42	4.59
21600.	13.3	16.7	11.6	16.1	14.1	15.6	12.1	15.9

Table 7.4

Forces in Chords and Diagonals from Theory and Experiment at the beginning and the end of loading on the truss.

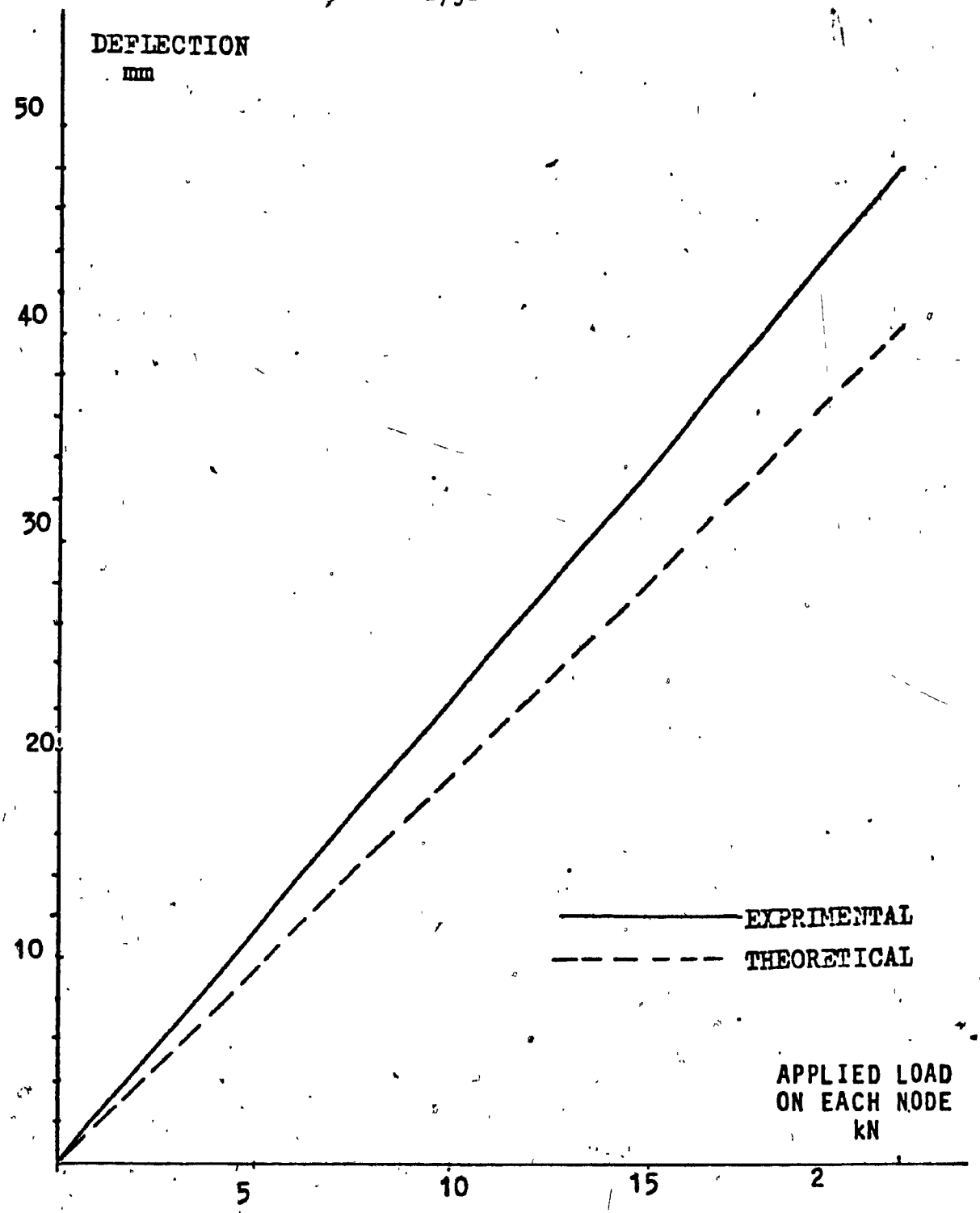

FIG. 7.6 LOAD-DEFLECTION CURVE FOR CENTRAL POINT OF THE TRUSS

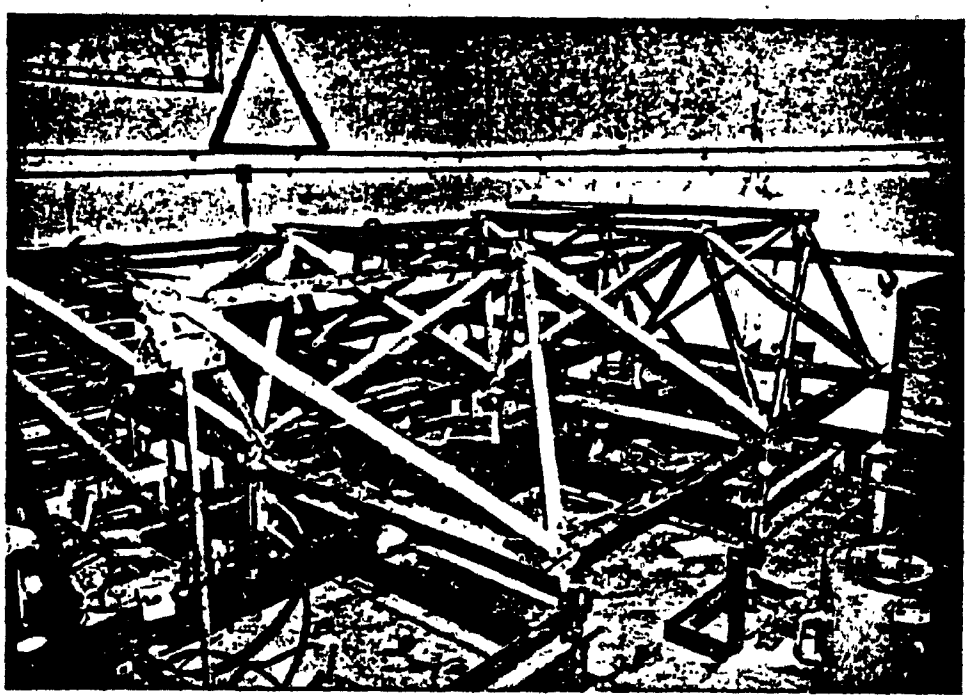

FIG. 9.7 TEST TRUSS

CHAPTER VIII

CONCLUSIONS

An eccentrically loaded strut (T-shape) has been studied. The load-shortening relationship in the elastic range is non-linear, the stiffness decreases with increasing force, and the bowing is gradual and quite noticable.

The use of T-shape diagonals gives a "quasi ductile" behaviour to space trusses which makes them safer and more controllable, while the distribution of moments and shear forces is made more uniform.

For an optimum truss employing heavy edge chords, an increase of 22% in load capacity was obtained by using T-shape diagonals (for the same chord size).

To demonstrate the influence of T-shape diagonals on behaviour of space trusses a small space truss was tested. The test results can be summarized as follows:

1. The diagonals in the truss bowed gradually, with midspan deflection of 20 mm at the maximum load, while still elastic.
2. The experimental relationship between applied load and internal forces in the diagonals differed somewhat from

the computer analysis, but the final force carried by the diagonals are in reasonable agreement.

3. The important result of the test was the demonstration that the middle chord and side chords carried almost equal load at the limiting capacity (computed ratio of 1.8:1 for concentrically loaded diagonals).
4. The experimental load capacity of the truss in the elastic range agreed with the computer analysis. This indicates that the equivalent area used for the T-shape diagonals was appropriate.

Suggestions for more research:

- Other types of section for eccentrically loaded struts need to be studied in respect to load-shortening relationships.
- The influence of T-shape diagonals on trusses which are supported over more than one span needs to be analysed.

REFERENCES:

[1] 'Second International Conference on Space Structures', University of Surrey, Guildford, England, Sept. 1975, ed. by R.M. Davis.

[2] Latticed structures "State of the Art Report", by the Task Committe on Latticed structures of the Committee on Metals, Journal of the Structural Division, ASCE. Vol. 102, No. ST 11 Nov. 1976, pp. 2197.

[3] Renton, J.D., "The Related Behaviour of Plane Grids, Space Grids and Plates" Space Structures, R.M. Davies, Ed., London, UK, 1966.

[4] Suzuki, E., Kitmarmaru, H. and Yamada, M., "The Analysis of the Space Truss Plate by Difference Equations", First International Conference on Space Structure, University of Surrey, England, ed. by R.M. Davis, 1966, pp. 136-144.

[5] Flower, William, R. and Schmidt, Lewis, C., "Analysis of Space Truss as Equivalent Plate", ASCE, J. Struct. Div. 97, ST 12, December, 1971, pp. 2777-2789.

[6] Flower, William R. and Schmidt, Lewis, C., "Approximate Analysis of a Parallel-Chord Space Truss", Institution of Engineers, Australia, Civ. Eng. Trans., CE-13, April, 1971, pp. 52-55.

[7] Dickie J.F. and Dunn, D.J., "Yield Pattern Considerations in Space Structures", J. Inst. Struct. Eng. 53, March, 1975, pp. 147-152.

[8] Mezzina, M., Prete, G. and Tosto, A., "Automatic and Experimental Analysis for a Model of Space Grid in Elastoplastic Behaviour", 2nd International Conference on Space Structure, University of Surrey, England, September 1975, pp. 570-588.

[9] Schmidt, L.C., "Alternative Design Methods for Parellel Chord Space Trusses", Structural Engineer (UK), Vol. 50, No. 8, August, 1972, pp. 295-302.

[10] Morgan, P.R., Schmidt, L.C., Coulthard, B.R., "The Influence of Eccentricity and Continuity on the Inelastic Behaviour of a Space Truss", 6th Australian Con. on the Mech. of Structures and Materials, Un. of Caterbery, Christchurch, N.Z., Aug. 1977, pp. 274-281.

[11] Schmidt, L.C., Morgan, P.R. and Clarkson, J.A., "Space Trusses with Brittle Type Strut Buckling", Journal of Structural Division, ASCE, Vol. 102, No. ST7, July, 1976, pp. 1479-1492.

[12] Wolf, J.P., "Post Buckled Strength of Large Space Trusses", Journal of the Structural Division, ASCE, Vol. 99, No. ST7, 1973, pp. 1708-1712.

[13] Zienkiewicz, O.C., et al, "Elasto-Plastic Solution of Engineering Problems, Initial Stress, Finite Element Approach", International Journal for Numerical Methods in Engineering, Vol. 1, 1969, pp. 75-100.

[14] Rosen, A. and Schmit, Jr., L.A., "Design Oriented Analysis of Imperfect Truss Structure Part 1 - Accurate Analysis", International Journal of Numerical Methods in Engineeriong, Vol. 14, No. 9, 1979, pp. 1309-1321.

[15] Schmidt, L.C. and Gregg, B.M., "A Method for Space Truss Analysis in the Post-Buckling Range", International Journal for Numerical Methods in Engineering, Vol. 15, No. 2, Feb. 1980, pp. 237-247.

[16] Marsh, C., "Orthogonal Grid Space Trusses: Ultimate Strength and Optimization", Second International Conf. on Space Structure, Un. of Surrey, England, ed. by R.M. Davis, 1975, pp. 550.

[17] Horne, M.R., "The Elastic-Plastic Theory of Compression Members", Journal of the Mechanics of Physics of Solids, Vol. 4, 1956, p. 104.

[18] Popov, E.P., "Mechanics of Materials", Second edition, Prentice-Hall, Inc., Engelwood Cliffs, New Jersey 07632.

[19] Marsh, C., "Strength of Aluminum", Alcan Canada Products Limited, Fifth edition, April 1983.

[20] Nicholas Iliadis, "Ultimate Strength of Orthogonal Grid Space Trusses", A thesis in Concordia University, November 1975.

[21] Marsh, C., "International Centre, Rio De Janeiro", ASCE Convention, New York, May, 1981.

[22] Marsh, C., "Collapse of Point Supported Square Grillages", Journal of the Structural Division, ASCE, Vol. 103, No. ST9, September, 1977, pp. 1703-1712,

[23] Chin Be, Y.K., "Automatic Limit Analysis of Triangulated Space Structures", J. Inst. Struc. Eng. 48, January, 1970, pp. 21-29.